THE DAMAGE-FAILURE CRITERIA FOR NUMERICAL STABILITY ANALYSIS OF UNDERGROUND EXCAVATIONS: A REVIEW

Shahriyar Heidarzadeh[1], Ali Saeidi[2], Alain Rouleau[2]

Correspondance

Shahriyar Heidarzadeh, Department of Applied Sciences, Université du Québec à Chicoutimi, Chicoutimi (Québec) G7H 2B1, Canada, Tel: +1 (418) 545-5011 ext. 2589, Email: shahriyar.heidarzadeh1@uqac.ca

Present address

Department of Applied Sciences, Université du Québec à Chicoutimi, Chicoutimi (Québec) G7H 2B1, Canada.

ABSTRACT

Failure of rock mass in deep underground excavations could be attributed to a broad range of performance malfunction, from plastic yielding of rock, generation of macro cracks on the boundary of the excavation, gravity driven rockfalls or even complete stress-induced collapse. The failure criteria determine the stress level (or strain level) at which the rock mass loses its load-carrying (or strain-carrying) capacity. Determination of the state of underground stability can be successfully achieved through implementation of appropriate failure criteria within the numerical analyses' tools. The choice of failure criteria in numerical stability analysis plays a key role in defining the behaviour of an underground excavation. A failure criterion will be useful only if selected based on the correct mechanism of failure. Plus, a right choice of failure criterion, significantly reduces the errors of quantifying an excavations behaviour. Therefore, this paper offers a critical review of the most common stress-based and strain-based failure criteria used in numerical stability analysis of underground excavations. Particular attention is paid to characterize different mechanisms of underground failure and recommendations are formulated for each failure mode. In addition, this paper addresses the theoretical considerations for the applicability of different failure criteria and highlights the practical limitations for their numerical implementation.

KEYWORDS: Rock Mass Failure; Underground Excavations; Stress-Based Criteria; Strain-Based Criteria; Numerical Modeling.

[1] Researcher in Rock Mechanics, Department of Applied Sciences, Université du Québec à Chicoutimi, Chicoutimi (Québec) G7H 2B1, Canada.

[2] Professor, Ing., Ph.D. Department of Applied Sciences, Université du Québec à Chicoutimi, Chicoutimi (Québec) G7H 2B1, Canada.

1. INTRODUCTION

The progression of underground mines to greater depths presents new challenges for the mining industry to ensure the safety of underground spaces and to maintain the productivity. Ensuring the safety of personnel and equipment in deep underground mines is linked with the implementation of suitable strategies to provide stability, all through the design, the planning and the production phases. Inappropriate design methodologies or ineffective geotechnical monitoring often leads to failure of underground excavations resulting in production delays, increased costs, or in some cases, termination of mining activity.

Rock mass instability around underground excavations can be characterized based on the *in situ* stress level and the rock mass quality. The rock mechanics engineers in a mine are challenged to predict when the damage process initiates within the rock mass, under which circumstances it leads to failure, and also what are the quantitative measures to differentiate between damage, yield or eventual failure. To answer these questions, rock mass deformation – failure mechanisms should be comprehensively studied, secondly suitable approaches to quantify the level of rock mass damage (e.g. empirical or numerical analysis approaches) should be identified, and finally the appropriate criteria must be adopted to determine whether the failure has occurred or not. The failure criteria will be useful, if they are based on the correct mechanism of failure.

As stated in the literature, state of stability in underground excavations can be successfully assessed through implementation of appropriate failure criteria in conjunction with numerical analysis methods. Even though conventional analytical and empirical approaches were used extensively in the past for stability evaluation purposes, some fundamental shortcoming and drawbacks have been identified associated to them. Actually, closed-form analytical solutions such as those provided by Kirsch (1898), Ladanyi (1974) and Brady and Lorig (1988) are only suitable to deal with simple geometries and may not offer satisfactory solutions with complex mining conditions (Zhang 2006; Sepehri 2016; Heidarzadeh 2018). On the other hand, the common empirical methods such as the Stability Graph Method developed by Mathews et al. (1981) and modified by Potvin (1988) are also suffering from limitations such as the lack of consideration for the mining method, they ignore the drilling and blasting effects, they neglect the geological structures, they oversimplify complex geometries and they are unable to predict gravity driven rockfalls and tensile mode of failure (wall relaxation) (Hutchinson and Diederichs 1996; Suorineni 2010; Idris 2014; Sepehri 2016). In addition, these methods only offer a qualitative measure of stability and their application is limited to real site-specific cases. Numerical methods circumvent the drawbacks of analytical and empirical methods since they are capable of solving complex mining problems, and also of incorporating different failure criteria corresponding to various mechanisms of failure. In fact, numerical methods are efficient tools for evaluating the state of excavations stability since they quantify the magnitudes of induced stresses within a given modeled region and they relate them to different levels of rock mass damage by using the failure criteria.

Literature is rich with studies that employed different existing failure criteria with numerical methods to evaluate the potential of rock mass instability in underground excavations. However, no comprehensive review has been published so far explaining the applicability of various failure criteria and providing guidance for the selection of

appropriate criteria for different instability mechanisms. In fact, there is a gap in the understanding between identifying different mechanisms of instability and selecting the most appropriate criteria to effectively address them. An in-depth review of the commonly used failure criteria in underground stability problems is needed to explain the theory behind each criterion and to describe their applications in numerical analysis for different underground instability problems. Filling this gap is crucial since a successful numerical assessment of underground instability is not achievable without an accurate identification of probable modes of failure, the employment of appropriate corresponding failure criteria to better reflect the rock mass behaviour, and finally a correct implementation of the failure criteria in conjunction with numerical analyzing tools.

The objective of the present paper is to provide a critical review of the existing stress-based and strain-based failure criteria used in numerical stability analysis of underground excavations. This review is focused on cases which use continuum numerical analysis and does not include the discontinuum behaviour of a rock mass. All the static and dynamic mechanisms of instability in underground excavations are described; however, only the non-dynamic failure criteria are furtherly covered. Moreover, this paper tries to provide guidance to the selection of the most appropriate failure criteria for different failure mechanisms. Finally, this paper highlights key points regarding the general application of each failure criterion, and it offers some useful remarks about their numerical implementation.

2. ROCK DEFORMATION PROCESS AND UNDERGROUND FAILURE MECHANISMS

Evaluation of underground excavations' stability requires knowledge of the failure – deformation process (i.e., stress–strain behaviour) of rock. Prior to excavation, the stress-strain behaviour of a rock mass is defined by its geological history. An excavation results in a volume of rock mass which was previously acting as a support to be removed. The disturbance caused by this partial removal of rock, creates deformations and develops fractures within the rock mass, resulting in minor to extensive damage/failure around the excavations periphery (Aglawe 1999; Souly et al. 2003; Brady and Brown 2004; Hidalgo 2013; Villaescusa 2014).

For an intact rock specimen, the failure–deformation behaviour under different loading and confinement conditions, can be classified as viscous elastic or plastic. The response of the rock specimen can also be characterized as linear or nonlinear, partly linear and partly nonlinear. The behaviour of rock and subsequent damage process is directly defined via the constitutive models of rock (Zhang 2006; Brady and Brown 2004). Constitutive models find a crucial application with different failure criteria. Hence, these models are further described here. The different stages of brittle failure–deformation process usually associated with strain-softening behaviour of the specimen is presented in Fig. 1 (Brady and Brown 2004; Hidalgo 2013).

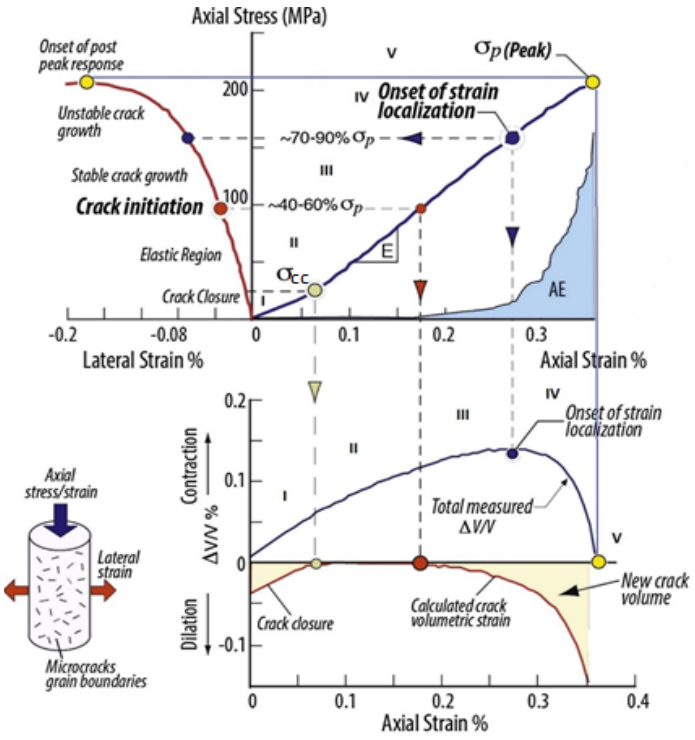

Figure 1- Progressive failure process of intact rock under compressive loading (adapted from Hoek and Martin 2014).

Viscous[3] constitutive models can simulate the behaviour of rock in the first stage where closure of pre-existing microcracks occur (Eberhardt et al., 1998; Cai et al., 2004; Zhang 2006; Hidalgo 2013). Elastic constitutive models[4] can be used to simulate the behaviour of rock where the elastic deformation and stable crack growth happen as a result of loading (Cai et al., 2004; Zhang 2006). Yield occurs eventually by unstable crack propagation as elastic behaviour changes to plastic behaviour [5] causing the permanent (plastic) deformations to appear (Brady and Brown 2004). Plastic models and/or viscous constitutive models can appropriately reflect the behaviour of rock in the peak and the post peak stages (Zhang 2006). The peak strength of the rock shows the onset of post-peak behaviour. Peak strength is defined as the maximum stress the rock can endure under a given set of confinement conditions (Zhang 2006; Brady and Brown 2004). Failure can be initiated or even occur at the peak strength, in some cases accompanied by extensive plastic deformation of the specimen (Brady and Brown 2004). Exceeding the peak strength, marks the transition from continuum to discontinuum behaviour. For laboratory specimens, the transition from continuum to discontinuum can be recognized by the formation of shear

[3] ln general, viscous behaviour, refers to the time-dependent behaviour of rock. Low quality and weak rocks, (such as sedimentary rocks), mostly show viscous behaviours before the linear elastic stage, and also after yielding, another stage of viscous behaviour (Zhang t2006; Brady and Brown 2004).

[4] The constitutive relation of elastic behaviour, if linear, is associated to Hooke's law; and if non-linear follows generalized Hooke's law (Zhang 2006; Brady and Brown 2004).

[5] Plastic behaviour of rock, can be grouped as perfectly plastic behaviour, hardening behaviour, and softening behaviour. If an increasing stress produces further post-yield deformation and higher residual strength, the rock exhibits strain-hardening behaviour. In contrast, strain-softening behaviour marks the decreasing resistance of a rock specimen to load, at increasing axial deformation (Brady and Brown 2004).

bands within the rock sample or by the deterioration and axial splitting. However, in field conditions, the transition from continuum to discontinuum around the excavation periphery occurs in the form of detached volumes of rock (i.e. spalling, slabbing or violent failure of rock) (Eberhardt et al., 1998; Aglawe 1999; Cai et al., 2004; Brady and Brown 2004).

Hoek et al., (1995) studied different possible failure mechanisms and instability modes in underground excavations under low and high *in situ* stress conditions and as a function of fracturing level of the rock mass. Later, Martin et al., (1999) incorporated the influence of the intermediate *in situ* stress as illustrated in Fig. 2 which is adapted from Kaiser (2020).

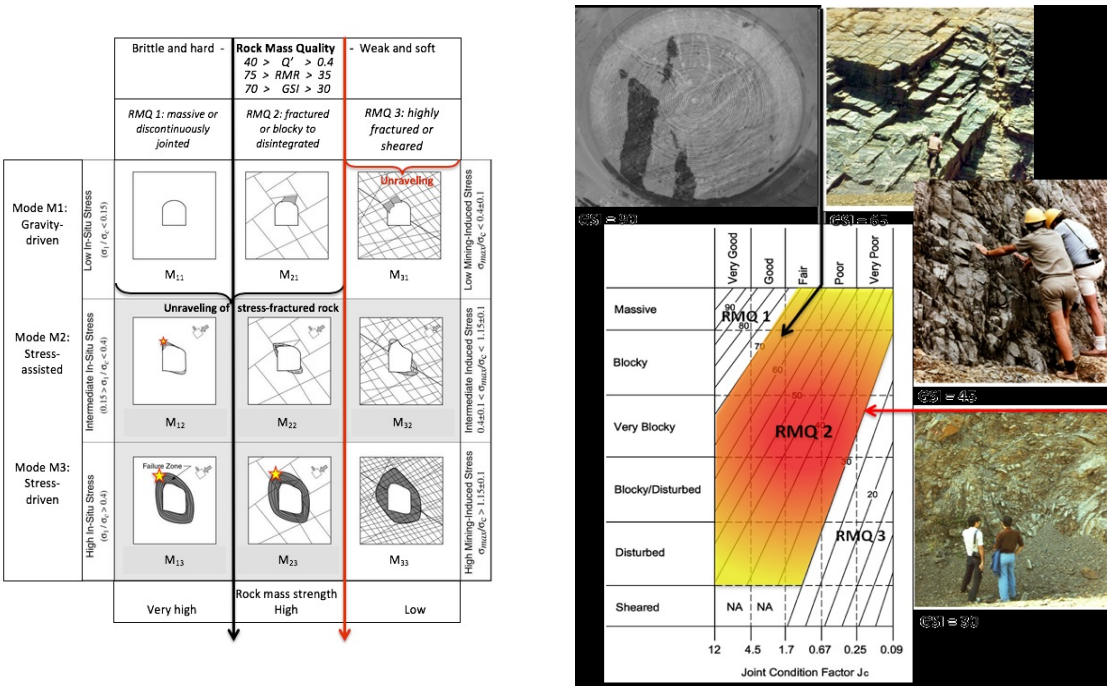

(a) (b)

Figure 2- (a) Excavation behaviour matrix based on rock mass quality (RMQ), and *in situ* stress state (presented in left vertical axis) or the mining-induced stress concentrations (presented by the stress level, on the right vertical axis), exemplifying different modes of rock mass failure including brittle failure (as highlighted grey rectangles) (b) the equivalent RMQ in the Geological Strength Index (GSI) chart (adapted from Kaiser (2020)).

Kaiser (2020), discussed the nine possible static failure modes (occur solely by static mining-induced stresses) of unsupported underground excavations in the context of excavation behaviour matrix (Fig. 2a). The excavation behaviour matrix categorized the static failure modes as a function of stress level (*SL*) and rock mass quality (RMQ) (Fig. 2b). The RMQ is specified based on the degree of fracturing within the rock mass and the *in situ* stress intensity near the excavation boundary. The *in situ* stress intensity is characterized as the ratio of maximum principal *in situ* stress to strength (σ_1/σ_c) and the mining-induced *SL* is assumed equal to $(3\sigma_1-\sigma_3)$/UCS. Kaiser (2020) remarked that the limits of RMQ in the behaviour matrix have been customized from Kaiser et al. (2000) according to the experiences with deep excavation failures.

According to the excavation behaviour matrix, at low *in situ* stress environments, the failure mechanism is mainly controlled by the distribution of discontinuities. As can be seen in Fig. 2a, in massive rock masses having a limited number of discontinuity sets and wide spacing between constituents of the sets, a linear elastic response would be expected from the rock mass (M_{11}). This type of rock mass should not require support or reinforcement to maintain stability during the excavation process (Villaescusa 2014; Martin 2019). However, for the excavation situated in fractured or blocky to disintegrated rock masses, falling or sliding of rock blocks and wedges could occur as the dominant failure mechanism (M_{21}). However, excavations situated in highly fractured rock masses would fail through the mechanism of blocks unraveling from the excavations surface (M_{31}).

By increasing the *in situ* stress level, fresh stress-induced fractures parallel to the excavation boundary will be created. At intermediate *in situ* stress levels, stress concentrates at distinct locations around the excavation boundary, resulting in localized brittle failure of intact rock which is considered as the dominant mode of failure for the high quality massive to discontinuously jointed rock masses (M_{12}) (Kaiser 2020). As can be seen in Fig. 2a, localized brittle failure could occur at one shoulder and the toe of the wall at opposite sides of the excavation. It is also probable that failure at the toe of the wall could undercut the overlying rock and propagate upward (Villaescusa 2014). In terms of excavation-induced stress level, localized brittle failure zones (also referred to as breakout or v-shaped notch) are mostly observed for the intermediate mining-induced stress levels where $SL \leq 1$. In fact, localized spalling or slabbing (brittle failure of intact rock) could be expected by exceeding the *SL* from 0.3 to 0.5 (M_{12}) (Bewick et al. 2019). Strainbursting has also the possibility of occurrence in high quality massive rock masses as remarked by the star sign in Fig. 2a. The localized brittle failure in the excavations located in moderately fractured rock masses are bounded by open discontinuities and joints, which facilitate movement of rock blocks near the excavations boundary (M_{22}) (Kaiser 2020). In fact, unraveling of rock blocks occurs if the shear strength of a joint face is being smaller than the shear stresses acting across the joint face and the orientations of the joint face is aligned to the orientation of the stresses (Villaescusa 2014). In the case that the joints do not slide, tensile cracks could be generated and furtherly propagate and coalesce to form blocks that slide. Ultimately, in highly fractured rock masses (RMQ3), the likelihood of blocks sliding/unravelling along discontinuities into the excavations void (M_{32}) increases especially since the fractured zone might be expanded over the entire boundary of the excavation (Golchinfar 2013; Hidalgo 2013; Kaiser 2020).

At high *in situ* stress conditions, excavations located in massive to discontinuously jointed rock masses will experience deep brittle failure of intact rock (spalling and slabbing) throughout the entire excavations surroundings (M_{13}) (Martin 2019; Kaiser 2020). Similar-to-intermediate *in situ* stress conditions, massive rock masses under high stress levels also have the potential of strainbursting on the excavations surface or at some distance from the surface (shown by the star sign in Fig. 2a) (Kaiser 2020). In the case of excavations located in fractured or blocky rock masses, brittle failure happens around the entire excavation area accompanied by movement of rock blocks along the open fractures (M_{23}). In fact, the rock mass behaviour is highly influenced by the orientations of the discontinuities relative to the stress components (Villaescusa 2014). Eventually, excavations placed in highly fractured or sheared rock mass context are failed through excessive stress-driven plastic

deformation/yield (M_{33}) (Martin 2019, Kaiser 2020). Failure will occur in the form of rock squeezing with or without swelling in an elastic/plastic continuum (Kaiser 2020).

In general, since the bedded rock mass mostly exist in shallow depths, and deep underground mines are usually located in a hard rock mass context, two main failure mechanisms were identified for deep underground mines, namely (1) structurally controlled gravity-driven; and (2) stress induced gravity-assisted failures (Bewick 2008; Martin 2019; Kaiser 2020).

Aside from static failure modes which are caused by excavation-induced stresses, dynamic failure modes in unsupported underground excavations occur as a result of dynamic loading from earthquakes or mining-induced seismic events (e.g. blasting). Dynamic disturbance in underground excavations fundamentally cause the same failure modes as static failure except that the dynamic loading changes the static forces, stresses and deformations as well as the deformation rates (Mah 1997; Cai et al., 2004; Golchinfar 2013; Kaiser 2020). Dynamic failure modes of rock could occur in two major forms of brittle unstable failures including (a) strainbursts sometimes with rock ejection caused by tangential straining (manifested in $M_{12\ to\ 13}$ and M_{23} in Fig. 3) (Aglawe 1999; Castro et al. 2012); and (b) seismically induced falls of ground or as stated by Kaiser (2020) shakedown failures (manifested in $M_{31\ to\ 33}$ and M_{22} to $_{23}$ in Fig. 3).

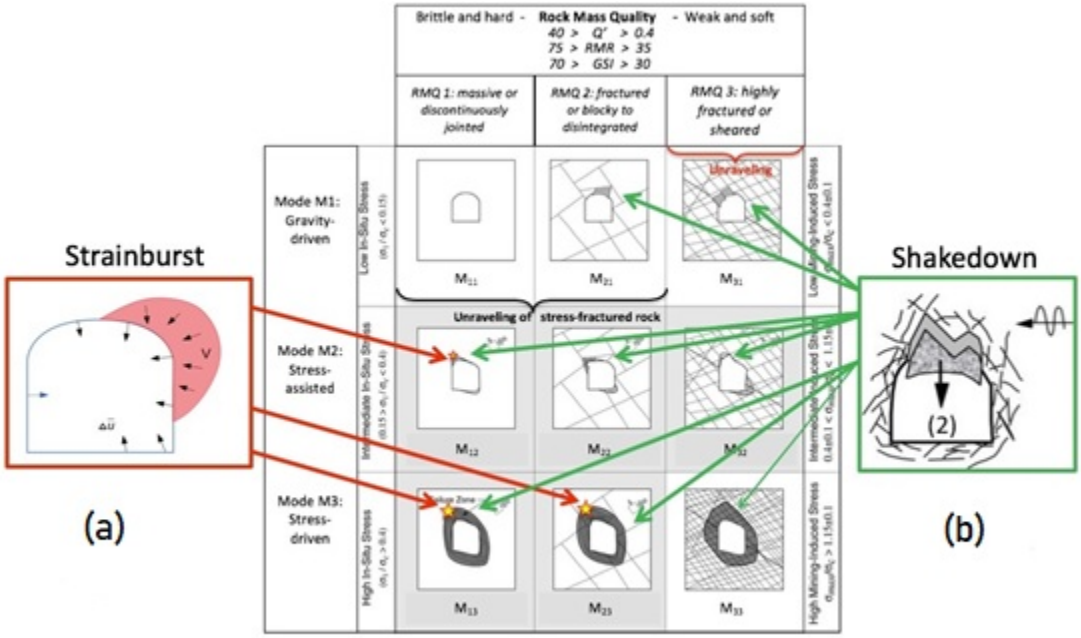

Figure 3- Two main dynamic failure modes illustrated in the excavation behaviour matrix: (a) strainburst, and (b) shakedown (adapted from Kaiser 2020).

A comprehensive explanation of the dynamic failure modes of rock mass is provided by Cai and Kaiser (2018) and Kaiser (2020), and readers should refer to these for further information. Dynamic modes of underground failure (rockbursts) are beyond the outlines of this research. The failure criteria reviewed further in this paper, are the static,

structurally-controlled, gravity driven, stress assisted and stress driven (non-dynamic) failure mechanisms, or a combination of them.

Once the underground failure modes and damage mechanisms are understood and identified, an appropriate constitutive models and failure criteria could help in characterizing the rock behaviour and determining the excavations performance.

3. FAILURE CRITERIA USED IN EXCAVATION DESIGN

The failure criterion in stability analysis terminology can be defined as a formula which indicates the stress (or strain) level at which the ultimate strength of the rock is reached. A failure criterion will be useful if it is based on the correct mechanism of failure. A failure mechanism characterizes the process leading to failure. However, failure is a generic term and a case-dependant factor that can be attributed to a range of the excavations performance malfunction, from plastic yielding of rock, generation of visible cracks on the boundary of the excavation, gravity driven rock falls or even complete stress-induced collapse (Edelbro and Sandström 2009; Idris 2014). A failure criterion quantifies the failure as a process under which rock mass loses its load (or strain)-carrying capacity by exceeding its response of interest (e.g. depth of yield, strain, convergence and others) from a predefined maximum tolerable threshold (Brady and Brown 2004; Kwasniewski and Takahashi 2010; Idris 2014; le Roux and Brentley 2018).

The failure criteria that are commonly used for numerical evaluation of the state of underground instability are categorized into two general groups, that are stress-based and strain-based criteria. A review on the most common criteria in each of the above-mentioned categories are provided in the following sections.

3.1 STRESS-BASED FAILURE CRITERIA

In underground stability problems, stress-based failure criteria are employed to evaluate the load-carrying capacity of rock masses in the vicinity of underground excavations (Kwasniewski and Takahashi 2010). The majority of the existing failure criteria are formulated in terms of stresses (Hidalgo 2013). Stress-based failure criteria can be described by the maximum principal stress (σ_1) that a rock can withstand for a given magnitude of intermediate (σ_2) and minimum principal stresses (σ_3) (Ulusay and Hudson 2007; Le Roux and Brently 2018). The use of stress-based failure criteria is suitable for situations where constitutive models could be assigned to rocks in numerical analysis (Edelbro 2003; Hidalgo 2013). An in-depth review of the most common stress-based failure criteria used in numerical analysis of underground openings are provided in the following sub-sections.

3.1.1 Strength-to-stress ratio (Factor of safety)

The strength-to-stress ratio is probably the most used criterion to evaluate the failure conditions for underground openings. The strength-to-stress ratio compares the rock mass strength with the magnitude of mining induced stresses by using failure criteria. The ratio

generates a factor of safety which typically ranges between 0 and 10 (Abdellah 2013). However, according to the plasticity theory, the failure criterion here can be considered as a yield surface which limits the stress condition corresponding to the ultimate failure of rock. Therefore, it is more reasonable to speak of "yielding" criteria instead of failure criteria. Different yielding criteria can be used to compare the stress level and the rock mass strength around underground excavations (Souley et al., 2003).

Some of the common yielding criteria in rock engineering are the Mohr-Coulomb criterion, Hoek-Brown empirical failure criteria (Hoek and Brown 1980), three-dimensional versions of the Hoek–Brown failure criterion such as Pan-Hudson criterion (Pan and Hudson 1988), Priest criterion (Priest 2005), Zhang-Zhu criterion (Zhang and Zhu 2007), as well as Drucker-Prager criterion (Drucker and Prager 1952), Rock Mass Bulking Model (RMBM) (Gomez-Hernandez and Kaiser 2003), Single hardening/softening constitutive model (Lade and Jackobsen 2002) and Cohesion-Weakening and Frictional-Strengthening model (CWFS) (Hajiabdolmajid et al., 2002).

Numerical implementation of strength-to-stress ratio requires the selection of a comprehensive constitutive model. Constitutive models are important since they define the mechanical behaviour of the rock by relating stress to strain. A comprehensive constitutive model involves a "flow rule" in addition to the failure (or yield) envelope to better explain the behaviour of rock at failure. Since, elasto-plastic numerical simulations allow continuation of the solution to post peak phase, the rock behaviour and consequently failure conditions would be subjected to change by either strain hardening or softening phenomena. The comprehensive behaviour of rock should be addressed by an elastoplastic constitutive model consisting of a linear and isotropic behaviour in the pre-peak region, non-linear peak strength behaviour, a hardening or softening post-peak behaviour based on a yield function and corresponding flow rule (e.g. associated flow rule), and usually a perfectly plastic behaviour in the residual phase. The post-peak behaviour of rocks is often associated to their quality. Average quality rocks tend to exhibit a strain softening behaviour after failure. While poor-quality rocks show an elastic-perfectly plastic behaviour. However, for hard, good quality rocks an elastic-brittle behaviour with a rapid drop of strength in plastic straining phase could be suitable (Cundall et al. 2003; Souley et al. 2003).

Although linear elastic models (isotropic, orthotropic and transversely isotropic models) could be useful in some simple problems, they are unable to give a precise description of the true stress state around underground openings; they normally show higher stresses than the rock mass strength (Zhang and Mitri 2008). On the other hand, plastic (elastoplastic) models are largely employed for numerical modelling of hard rocks since they are capable of reflecting the true elastic / plastic behaviour of rock under loading conditions. The most common elastoplastic yielding criteria implemented in numerical solutions, are Mohr-Coulomb, Drucker-Prager and Modified Hoek-Brown models. It should be noted that the Mohr-Coulomb and Hoek-Brown criteria are two-dimensional criteria in which the intermediate principal stress value is not being considered. However, three-dimensional criteria such as the 3D Hoek-Brown, the Zhang-Zhu, the Pan-Hudson, the Priest, the Simplified Priest and the Drucker-Prager criteria, consider the influence of the intermediate stress value (Zhang 2006; Le Roux and Brentley 2018; De Santis 2019). Moreover, the cohesion-weakening and friction-strengthening (CWFS) model developed by Hajiabdolmajid et al. (2002) is reported to show a good accuracy for prediction of the

brittle rock failure depth (Hajiabdolmajid et al. 2002; Edelbro 2008). Diederichs (2007) used the mode of instantaneous cohesion-weakening and friction-strengthening model based on Hoek-Brown failure criterion, and successfully predicted the geometry of the failed zone around a circular excavation in brittle rock (Golchinfar 2013).

Strength-to-stress ratio (i.e. factor of safety) has been extensively used in numerical stability analysis of underground openings. The factor of safety for the rock mass surrounding an underground excavation, can be simply defined as the ratio of stress over the peak strength of rock. It is noted in several studies that the common practice in underground rock engineering problems relating to factor of safety (FS), is to consider the values of FS > 1 as representing the stable conditions for an underground excavation; while FS = 1, represents the critical state between stable and unstable conditions, and the values of FS < 1, is considered as "failed" conditions for the excavation (Zhang and Mitri 2008; Abdellah 2013; Itasca 2014). However, as a more conservative approach due to ever present uncertainties, the critical threshold for the factor of safety is considered to be 1.3 or 1.4 instead of unity in multiple studies (Abdellah 2015, Nuang et al., 2018; Liang et al., 2019).

In the case of excavations wall relaxation (Diederichs 1999) as the cause of a common mode of instability (tensile failure) in low compressive-tensile stress state, strength-to-stress criterion is defined by comparing the magnitude of the minimum principal induced stress with the tensile strength of the rock mass (Heidarzadeh et al. 2018b). Regardless of the value of the major principal induced stress (σ_1), if the magnitude of minor principal induced stress (σ_3) exceeds the tensile strength of the rock mass, a failed condition would be considered. In some studies, rock mass is assumed with minimal strength against tensile stress, therefore the values of minor principal induced stress equal or below zero within the rock mass would lead to failure ($\sigma_3 \leq 0$) (Shnorhokian et al. 2015).

Literature is rich of studies using strength-to-stress ratio or the factor of safety in various domains of underground stability analysis (Zhang and Goh 2012; Idris 2014; Abdellah 2015; Shnorhokian et al., 2015, 2018; Heidarzadeh et al., 2018a, 2018b, 2019; Naung et al., 2018; Liang et al., 2019).

3.1.2 Stress concentration factor (induced stress level criterion)

The potential of compressive failure in zones of low compressive and tensile stresses can be evaluated with the stress concentration factor (*SCF*). The *SCF* is defined as the ratio of the major principal induced stress (σ_1) to the uniaxial compressive strength of the intact rock (*UCS*) as presented in equation 1 (Obert et al., 1960; Hoek and Brown 1980; Zhang 2006; Shnorhokian et al., 2018).

$$SCF = \frac{\sigma_1}{UCS_{intact}} \quad (1)$$

The value of *SCF* can be used to determine the location and extent of the zones under high compressive stress around an underground excavation (Zhang 2006). This criterion is suitable to simulate the loading mechanism of an unconfined compression test, therefore can indicate the zones within which the compressive stress exceeds the rock strength

(Shnorhokian et al., 2018). If the *SCF* value in a particular zone around an excavation is largely greater that unity, the zone can be considered unstable and prone to failure; however, if the *SCF* around an excavation has a more or less uniform distribution, such excavation is considered more stable (Obert, et al., 1960). The *SCF* criterion can be particularly used in linear elastic analyses as a powerful indicator of potential compressive failure (Zhang 2006).

The application of stress concentration failure criterion has been addressed by different studies in numerical stability analysis of underground excavations (e.g. Kumar 2003; Zhang and Mitri 2008; Abdellah 2015; Shnorhokian et al., 2018; Abdellah et al., 2018).

3.1.3 Failure criteria for brittle failure of rock

In brittle rock mass context, increasing the deviatoric loading ($\sigma_1 - \sigma_3 / UCS_{intact} \sim 0.6$ to 0.8) develops Griffith-type extension fractures within the rock, resulting in specific zones of potential rock mass failure (Castro et al., 2012; Kaiser 2020). At low confinement, fracture propagation which leads to rock mass spalling, continues since it is not suppressed by the existing level of confinement; while increasing the confinement level, increases the apparent cohesion, but may causes shear failure within intact rock. This transition in conditions, is represented by a sigmoidal (*S*-shaped) failure envelope (Fig. 4) in a multi-behavioural stress space (Kaiser 2016, 2019). The failure envelope is tri-linear and is depressed in the low confinement zone (Gao et al., 2019). Low confinement area (at the left side of the spalling limit), is where spalling and slabbing dominates; and high confinement area (right side of the spalling limit) is where shear failure mechanism dominates (Castro et al., 2012; Kaiser 2020). Depending on the dominant failure mechanism, the rock mass around an underground excavation can be divided into 'inner' and 'outer' shell zones. The spalling limit (shown in Fig. 4), separates the inner and outer shell instability environments. Inner shell instability problems (rock mass skin damage) are governed by the behaviour of the rock mass in the immediate vicinity of an excavation at low confinement conditions, i.e. in the zone where stress-fracturing can occur and cause breakage of blocks or fragment subparallel to the excavation boundary. On the other hand, outer shell instabilities at moderate to high confinement conditions, include problems which occur due to shear failure mechanism with kink-band formation and shear through intact rock such as pillar bursting or fault slip type problems (Castro et al., 2012; Gao et al., 2019; Kaiser 2020).

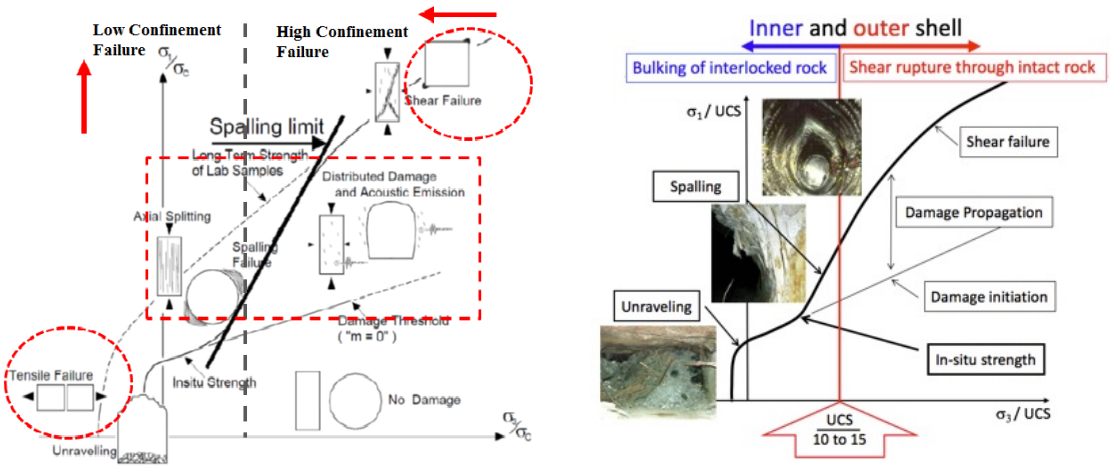

Figure 4- Sigmoidal *S*-shaped failure criterion for brittle rock masses divided into low and high confinement behavioural regions with illustration of different inner and outer shell instability problems (after Castro et al., 2012; Kaiser 2020).

The brittle shear ratio (BSR) is a differential stress criterion developed to assess the effect of mining-induced stresses on the inner shell stability problems of brittle rock mass surrounding deep underground excavations (Martin et al., 1999; Castro et al., 2012; Shnorhokian et al., 2015). The potential of strainbursts can also be addressed by using this criterion, as it compares the differential mining-induced stress ($\sigma_1 - \sigma_3$) around an underground excavation to the unconfined compressive strength (*UCS*) of the intact rock (Castro et al., 2012; Shnorhokian et al., 2015). Conceptually, this criterion can be defined through the notion of maximum shear stress since according to the Mohr Circle, the maximum shear stress within the rock is equal to the half the differential stress value. Therefore, the BSR can also be defined based on the maximum shear stress of the rock. The value of BSR can be calculated using the formula presented in equation 2.

$$BSR = \frac{(\sigma_1 - \sigma_3)}{UCS_{intact}} \qquad (2)$$

The intensity of rock mass damage can be categorized based on the normalized deviatoric stress levels (BSR value). As a design tool, rock mass damage initiation (DI) limit around deep underground excavations can be associated to the BSR value ranges approximately between 0.4 to 0.5; the BSR value above the threshold equal to 0.7 indicates major rock mass damage and the occurrence of failure due to strainbursting (Castro et al., 2012). The level of rock mass damage and the associated BSR level is tabulated as presented in Table 1.

Table 1- The level of rock mass damage and the potential of strainbursting (adapted from Castro et al., 2012)

$(\sigma_1 - \sigma_3)$ / UCS	Damage intensity	Strainburst potential
0.35	No to minor	No
0.35 to 0.45	Minor (spalling)	No
0.45 to 0.6	Moderate (breakout formation)	Minor
0.6 to 0.7	Moderate to major	Moderate
> 0.7	Major	Major

The Potential Stress Failure (*PSF*) criterion (formulated as $PSF = (\sigma_1/UCS_{rm}) \times 100$ by Mitri 2007), is a criterion similar to the BSR. The *PSF* is estimated at the boundary of an underground excavation, where minimum principal induced stress disappears. The maximum induced boundary stress (σ_1), can be obtained from numerical modelling and be compared with the *UCS* of rock mass.

The application of BSR in numerical stability analysis of underground openings has been examined by several recent studies (such as Abdellah 2013; Shnorhokian et al., 2015, 2018; Heidarzadeh et al., 2018a, 2018b and 2019).

3.1.4 Depth of yield zone

The depth or the extent of a yield zone, is probably the most popular instability indicator in numerical stability analyses. This is because continuum elastoplastic numerical models typically display indicators of yield and therefore can be used to establish the depth or extent of yield zones around an underground excavation (Zhang and Mitri 2008; Kaiser 2020). The yield condition (as a significant factor contributing to failure occurrence) happens at a point where the stress state satisfied the yield function (e.g. Mohr-Coulomb yield function) (Zhang and Mitri 2008; Abdellah et al., 2018). However, yielding of rock does not always lead to failure. Even though yield condition usually signifies the occurrence of plastic flow, it can also be possible that rock reaches the yield condition without any significant flow taking place. Kaiser (2020) stated that the rock surrounding an underground excavation can sustain its cohesive strength while yielding, and not falling apart or fail under gravity loading alone, i.e. will not unravel. However, in some cases where the yield in tension near the excavation boundaries led to the complete lost of cohesion, unsupported rock would unravel. Kaiser (2020), emphasized that the depth of yield is not necessarily the same as the depth of failure and a distinction should be made by considering the whole pattern of plasticity and the developed mechanism of yield (see Fig. 5).

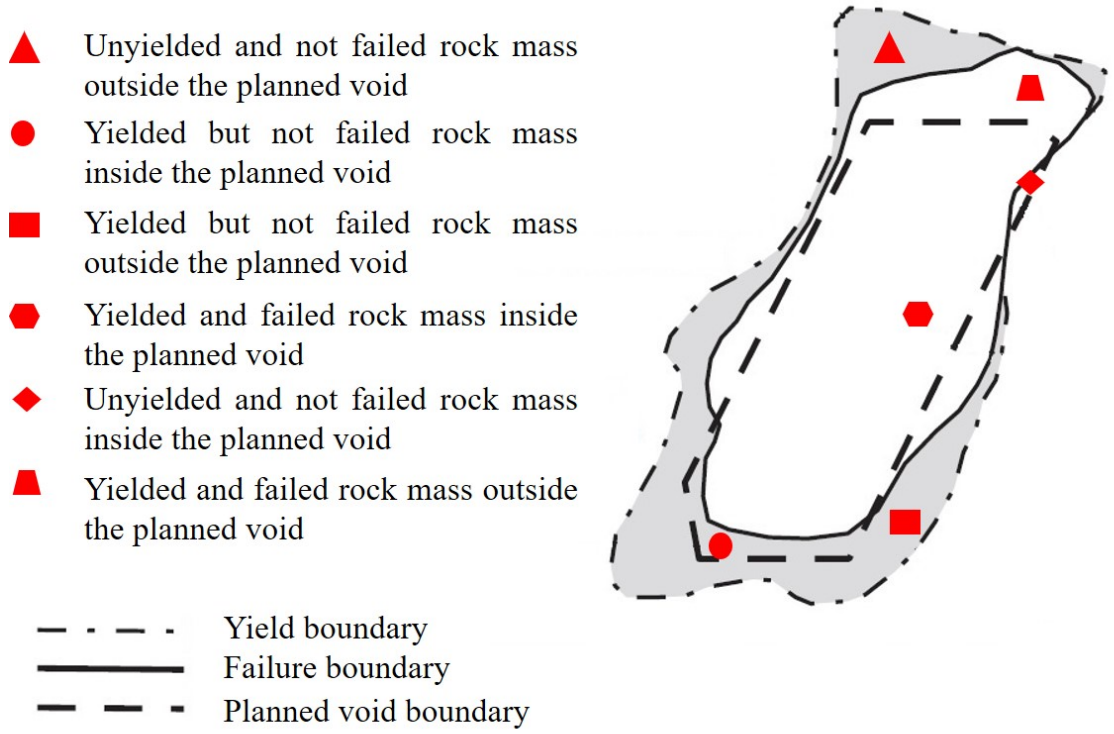

Figure 5- Illustration of possible yielded and failed rock mass around an open stope in relation to the planned and unplanned void geometry (adapted from Villaescusa 2014)

The depth of a yield zone as a criterion to evaluate the state of failure has been extensively applied in tunnel, cavern, drift and stope stability problems (Chen et al., 1983; Zhang and Mitri 2008; Valley et al., 2010; Wei 2010; Purwanto et al., 2013; Abdellah 2015, 2018).

3.1.5 Depth of failure

The depth of failure for an underground excavation, is defined as the difference in dimensions from a design surface to a resulting wall after a complete void creation. The estimation of the probable volume of failure for a specific area around an excavation, would necessitate to determine the *in situ* stress state as well as the rock mass strength and stiffness. Numerical analysis can provide the stress distributions around the excavations with any shape. Moreover, numerical analysis would allow incorporation of appropriate strength/failure criteria to estimate the depth of failure (Cepuritis et al., 2011; Villaescusa 2014).

According to Kaiser (2020), the extreme (maximum) depth of failure in unsupported rock mass can be defined empirically in relation to the calculated stress level *SL*, based on observations of the 'extreme' depth of failure (spalling). The extreme depth of failure (d^e_f) corresponds to the depth recorded at locations with the deepest or the most extreme failure (Gao et al., 2019). It was mentioned that the normalized extreme depth of failure (d^e_f/a)

for underground tunnels, increases linearly as a function of the stress level according to the formula provided in equation 3 (up to $SL \leq 1$ and at a lesser slope of 0.75 to a maximum at $SL = 1.5$):

$$\frac{d^e{}_f}{a} = 1.25SL - 0.51 \pm 0.1 \quad (3)$$

Where a is the tunnel radius. Kaiser (2020) also presented an approximate estimate of the mean depth of failure ($d^m{}_f$), based on the calibrated numerical modeling provided by Perras and Diederichs (2016) (see equation 4). According to Gao et al. (2019), the mean depth of failure is the average depth expected over a domain of uniform ground but with variable strength parameters (Gao et al., 2019).

$$d^m{}_f \approx \frac{d^e{}_f}{3.5 to 4.5} \quad (4)$$

Depending on the variability of stress and strength within the rock mass along a tunnel axis, the depth of failure could range from zero to $d^e{}_f$ (Gao et al., 2019; Kaiser 2020).

The above-mentioned relations can be used to anticipate the mean and extreme depths of failure in brittle rock masses. Other attempts have been made to develop different relations estimating the depth of failure around underground openings. In this regard, Beck and Duplancic (2005) determined the stresses using a nonlinear stress analysis and defined the depth and volume of failure considering the calculated plastic strains (Villaescusa 2014). Similarly, Cepuritis et al. (2007) used back analysis on the stope performance in Kanowna Belle Gold mine, with the purpose of quantifying the effect of induced stresses on the rock mass damage level. Subsequently, the obtained depth of failure contours was plotted in σ_1 - σ_3 space for two different rock mass qualities. The results were also subdivided into regions according to the probable experienced stress paths. It was demonstrated that the onset of increased depth of failure for massive to moderately jointed rock mass (Fig. 6a), exhibit good correlation with an estimated Hoek–Brown strength envelope (Cepuritis et al., 2007).

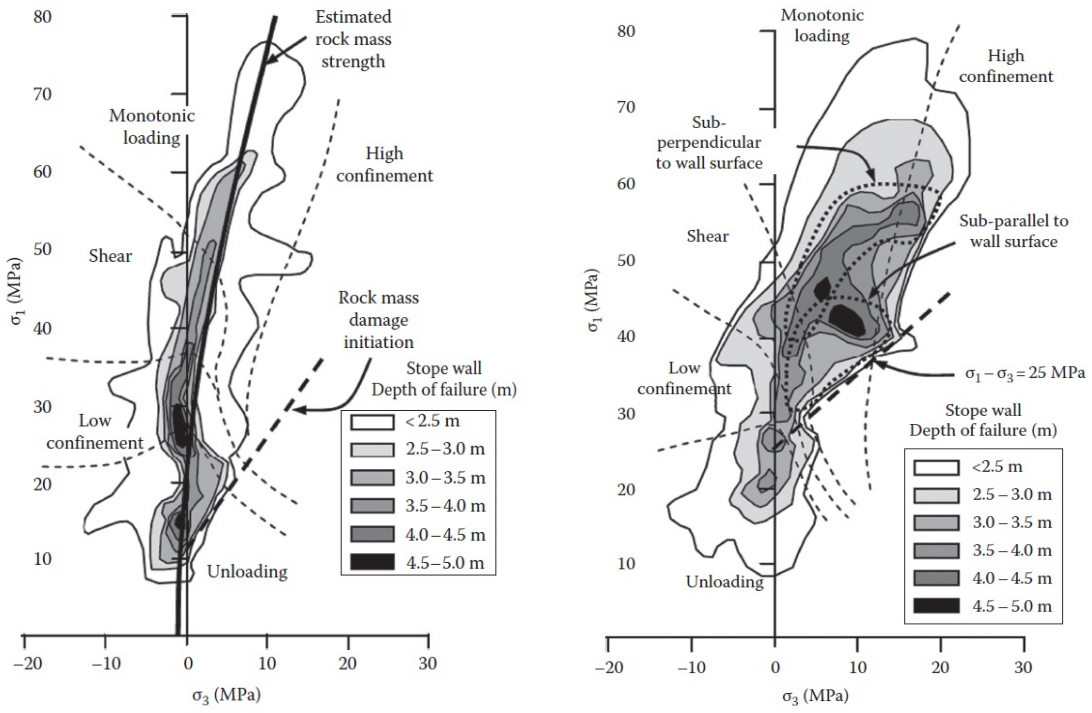

(a) (b)

Figure 6- Contours of depth of failure plotted in $\sigma_1 - \sigma_3$ space in a (a) massive to moderately jointed rock mass and (b) highly jointed rock mass (adapted from Villaescusa 2014)

Moreover, it was shown by Cepuritis et al., (2007) that the depth of failure increases with increasing stress in the form of changing the stress path from monotonic loading and shear towards low confinement conditions. Plus, the rock mass falloff occurs under unloading conditions, near the region of rock mass damage initiation threshold. However, for highly fractured rock masses (Fig. 6b), it was demonstrated that the depth of failure generally varies over a wider range of stress conditions (Cepuritis et al., 2007).

These semi-empirical indicators for the depth of failure could be integrated in numerical analyses tools to quantify the extent of rock mass damage and failure around underground excavations. The depth of failure as a stability indicating criterion, has been extensively employed in numerical stability analyses for different types of underground openings (Cepuritis et al., 2007; Ghasemi 2012; Abdellah et al., 2018; Oniyide and Idris 2019).

In the case of brittle failure of a rock mass, the depth of strainbursting could also find meaning as a failure criterion. Kaiser (2020) stated that although the depth of strainbursting is difficult to predict and quantify, it can be expected at locations of stress raisers, normally at the outer limit of the inner shell, around an excavation. For instance, in the case of a tunnel, strainbursting can easily involve 25% to 35% of the tunnel radius (Kaiser 2020). It was stated by Kaiser that the depth of strainbursting falls somewhere between d^m_f and d^e_f according to the equations 3 and 4. In fact, Kaiser (2020) mentioned that near zero depth of strainburst is expected for the tunnels in gradually spalling ground; while for typical tunnel sizes in massive to moderately (unfavorably) jointed ground, depths of 1 to < 2 m must be expected.

3.2 STRAIN-BASED FAILURE CRITERIA

Utilization of stress-based failure criteria is not always reasonable and / or justified. For instance, in some underground stability problems, the selection of an appropriate constitutive model for the rock is difficult due to lack of enough reliable data; or in some problems, assessing rock deformations is more convenient using proper measurement tools or even empirical methods. In such occasions, strain failure hypotheses could find application and the corresponding strain-based failure criteria can be employed to evaluate the state of rock mass stability (Kwasniewski and Takahashi 2010; Le Roux and Brentley 2018). Several strain-based criteria are commonly used in conjunction with numerical analyses tools. An in-depth review of these failure criteria is presented in the following sub-sections.

3.2.1 Stacey's extension strain criterion for fracture initiation in brittle rocks

Stacey (1981) proposed a criterion to predict and interpret the mechanism of fracture initiation in seemingly strong rocks under low confinement conditions (e.g. near the excavation boundary) (Wesseloo and Stacey 2016). The extension strain criterion successfully predicted both the orientation and the extent of fracturing in the sidewalls and face of tunnels prior to slabbing and spalling failure (Kwasniewski and Takahashi 2010; Hidalgo 2009, 2013).

According to this criterion, fracture initiation within brittle rocks occur when the total extension strain equals or exceeds a critical value which inherently is dependant on the rock properties (Kwasniewski and Takahashi 2010; Hidalgo 2013). The criterion can be expressed as follows (equation 5):

$$\varepsilon_e \geq \varepsilon_{ec} \quad (5)$$

Where ε_e is the extension strain and ε_{ec} is the critical or limiting value of extension strain of the rock (Kwasniewski and Takahashi 2010; Wesseloo and Stacey 2016).

The critical values of extension strain corresponding to the commencement of dilatancy, were determined by Stacey based on the experimental test results obtained for several rock types. Accordingly, the critical value of extension strain under uniaxial compression conditions, occurred at a stress level equal to about 30% of the rock strength (Stacey 1981; Kwasniewski and Takahashi 2010).

The Stacey's criterion has been used in several studies to characterize the stress-driven fractures around underground opening (e.g. Steffanizzi et al., 2007; Louchnikov 2011).

3.2.2 Sakurai's critical strain criteria

Sakurai (1981) devised a method called the "Direct Strain Evaluation Technique" to assess the stability of underground openings without requiring any stress analysis. In this

technique, the state of stability is determined through comparing the maximum principal strain (ε_1) in the vicinity of an excavation (obtained from displacement measurements) with an allowable threshold value of strain (called critical strain) (Fig. 7).

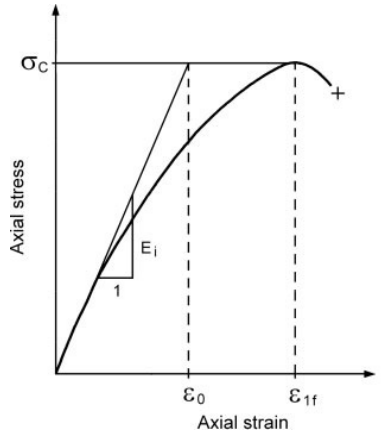

Figure 7- The notion of critical strain and strain at failure (adapted from Kwasniewski and Takahashi 2010).

Critical strain (ε_0), was calculated as the ratio of uniaxial compressive strength of rock by the Young's modulus as provided in equation 6 (Kwasniewski and Takahashi 2010):

$$\varepsilon_0 = \frac{\sigma_c}{E_i} \quad (6)$$

Technically, the critical strain may be different from the strain at failure strength for most rocks. Sakurai (1981) proposed a formula relating the strain at failure strength, to the critical strain as presented in equation 7.

$$\varepsilon_f = \frac{\varepsilon_0}{1 - R_f} \quad (7)$$

where ε_f is the strain at failure strength and R_f is a parameter representing failure strength. Sakurai (1981) mentioned that R_f values for a number of rocks and soils (from weak soils to hard rocks) varies between 0.005 to 0.8; however, according to Cai et al. (2011) R_f values are ranging between 0.1 to 0.3 for most hard rock masses. Based on the results of the laboratory test conducted on several rock and soil types, Sakurai concluded that critical strain ranges from 0.1 to 1.0% for rocks, and from 1.0 to 5.0% for soils with a uniaxial compressive strength ranging from 0.02 to 200MPa (Kwasniewski and Takahashi 2010).

Sakurai et al., (1993) later modified the critical strain criterion to take into consideration the possible shear failure mechanism of rocks around the underground openings by incorporating the shear strain. The new criterion evaluates the state of stability by using the maximum shear strain (γ_0) as presented by equation 8:

$$\gamma_0 = \frac{\tau_{\max}}{G_{50}} \quad (8)$$

where τ_{max} is the maximum shear strength, and *G50* is the shear modulus at 50% of τ_{max} (Fig. 8).

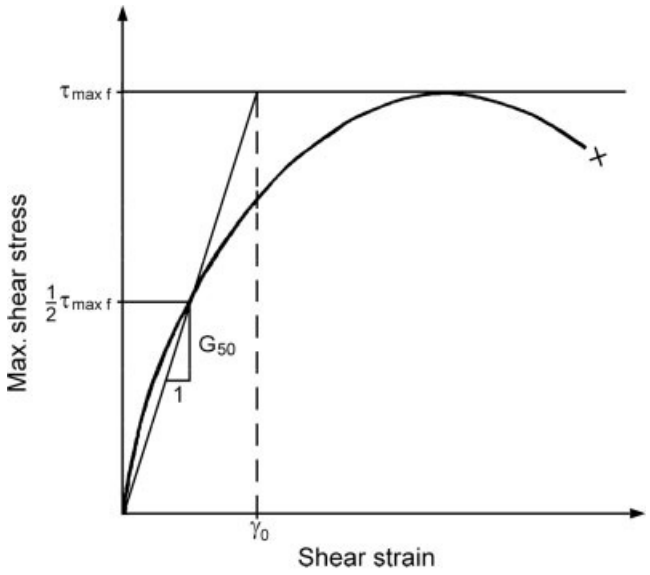

Figure 8- Explanation of critical shear strain (γ_0) in the stress – strain space (adapted from Kwasniewski and Takahashi 2010).

The criterion was re-formulated for isotropic materials as equation 9:

$$\gamma_0 = (1+\nu)\varepsilon_0 \quad (9)$$

where υ is the Poisson's ratio, and ε_0 is the critical normal strain. The allowable threshold value of the maximum shear strain could be determined from the uniaxial or triaxial compression tests through the formulas provided in equations 10 and 11.

$$\tau_{\max f} = \frac{\sigma_c}{2} \quad (10)$$

$$\tau_{\max f} = \frac{(\sigma_1 - \sigma_3)_f}{2} \quad (11)$$

where $\tau_{max\ f}$ is the maximum shear stress at strength failure.

Based on the results of uniaxial and triaxial compressive laboratory tests on some rock and soil samples, Sakurai (1993) has shown that most of the obtained data (in the critical shear strain / shear modulus space) lie between the two limiting boundaries as illustrated in Fig. 9. The transition line between the limiting boundaries could mark the evolution from the stable to the unstable state. The equations for the upper limit (γ_{UL}),

transition line (γ_T) and lower limit (γ_{LL}) in terms of critical shear strain and shear modulus are formulated as follows (equations 12-14) (Idris 2014):

$$\gamma_{UL} = 9.506G^{-0.3} \quad (12)$$

$$\gamma_T = 3.927G^{-0.3} \quad (13)$$

$$\gamma_{LL} = 1.516G^{-0.3} \quad (14)$$

The shear modulus (G) is determined using the equation 15:

$$G_{50} = \frac{E_{50}}{2(1+\nu)} \quad (15)$$

Where, *G50* and *E50* represent respectively the secant moduli of shear and longitudinal elasticity, at 50% of the ultimate strength; and ν is the Poisson's ratio.

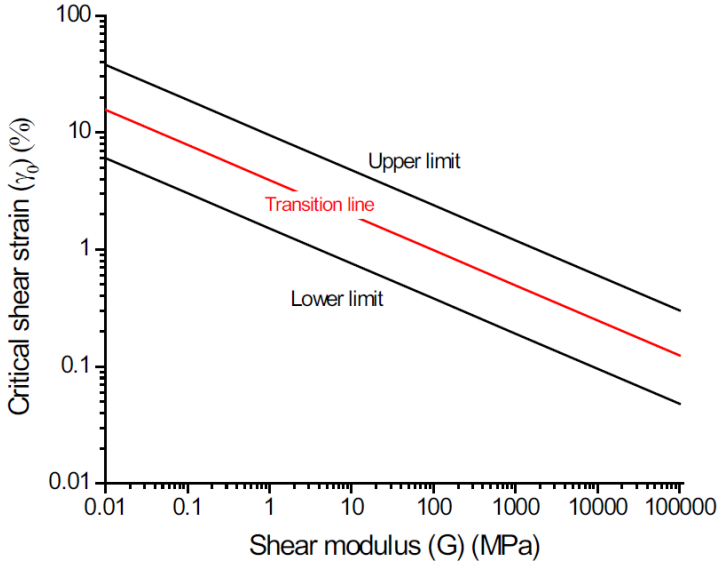

Figure 9- The limiting boundaries of stability explained based on critical shear strain and shear modulus (adopted from Idris 2014)

The Sakurai's critical strain criteria has been used in multiple studies to evaluate the yield/damage state of underground openings (Sahebi et al., 2010; Hidalgo 2013; Wengang 2013; Idris et al., 2015).

3.2.3 Aydan's strain criterion for squeezing evaluation

Aydan et al. (1993) have suggested a strain-based criterion based on the experiences obtained from case histories in Japan, firstly to evaluate the squeezing potential of tunnels. The method was developed on a basis of a closed form analytical solution generated between the axial stress-strain response of rocks in laboratory tests and the tangential

stress-strain response of rocks surrounding tunnels. The tangential strain of tunnels and the elastic strain limits of rock mass can be calculated as presented in equations 16-17.

$$\varepsilon^{e}_{\theta} = \sigma_{cm} / E_m \quad (16)$$

$$\varepsilon^{a}_{\theta} = \sigma_{\theta} / E_m \quad (17)$$

where, ε^{a}_{θ} is the tangential strain around a circular tunnel and ε^{e}_{θ} is the elastic strain limit of the rock mass; E_m represents the deformation modulus, σ_{cm} is the uniaxial compressive strength of the rock mass; and σ_{θ} stands for the maximum tangential stress applied on the tunnel walls.

The normalized strain levels are defined by the following equations (equations 18-20):

$$\eta_p = \varepsilon_p / \varepsilon_e = 2\sigma_{ci}^{-0.17} \quad (18)$$

$$\eta_s = \varepsilon_s / \varepsilon_e = 3\sigma_{ci}^{-0.25} \quad (19)$$

$$\eta_f = \varepsilon_f / \varepsilon_e = 5\sigma_{ci}^{-0.32} \quad (20)$$

where ε_e, ε_p, ε_s and ε_f are the absolute strains during the elastic, plastic, weakening and flowing stages (after yield point) of rock, respectively (Aydan et al. 1993; Hidalgo 2013). Accordingly, Aydan et al. (1993) proposed five different classes for assessing the squeezing potential as follows (from Hidalgo 2013; Ajalloeian et al., 2017):

(i) **No squeezing** (i.e. the rock exhibits elastic behaviour and the tunnel walls are stable): $\boldsymbol{\varepsilon^{a}_{\theta} / \varepsilon^{e}_{\theta} \leq 1}$;

(ii) **Light squeezing** (i.e. the strain-hardening behaviour is observed for the rock, however, the tunnel will remain stable): $\boldsymbol{1 < \varepsilon^{a}_{\theta} / \varepsilon^{e}_{\theta} \leq \eta_p}$;

(iii) **Fair squeezing** (i.e. the rock shows a strain-softening behaviour with a larger displacement): $\boldsymbol{\eta_p < \varepsilon^{a}_{\theta} / \varepsilon^{e}_{\theta} \leq \eta_s}$;

(iv) **Heavy squeezing** (i.e. a strain-softening behaviour is observed at a very high rate resulting in large displacements in tunnels): $\boldsymbol{\eta_s < \varepsilon^{a}_{\theta} / \varepsilon^{e}_{\theta} \leq \eta_f}$;

(v) **Very heavy squeezing** (i.e. collapse of the tunnel will occur due to flow of rock and heavy rock supports are required): $\boldsymbol{\eta_f < \varepsilon^{a}_{\theta} / \varepsilon^{e}_{\theta}}$.

A few other common approaches are used for evaluating the squeezing potential in underground excavations (particularly tunnels) as semi-empirical methods (e.g. Jethwa et al. 1984; Hoek and Marinos 2000) and theoretical-analytical approaches (e.g. Barla 1995) (Ajalloeian et al., 2017). However, compared to the empirical stress-based criteria, Aydan's criterion performed much better than the Hoek-Brown criterion in representing the whole range of experimental results. Moreover, Aydan's criterion provides the most appropriate continuous best fit to experimental results and bi-linear Mohr-Coulomb criterion. Besides, it shows an acceptable applicability to both brittle and ductile rock failure (Aydan et al., 2012).

Application of Aydan's criterion to evaluate the squeezing potential of underground spaces has been addressed in several studies (e.g. Singh et al., 1997 and 2007; Hidalgo 2013; Roache 2016; Ajalloeian et al., 2017).

3.2.4 Geometric bulking of stress-fractured rock

Stress-fractured ground with strong fragments of rock inside the inner shell will bulk, if deformed by tangential straining, and its volume will increase because of the unfitted geometry of the rock fragments. Occurrence of this phenomenon at the boundary of an excavation, results in unidirectional bulking of rock into the excavation void which is controlled by the excavation geometry and the imposed tangential strain (Fig. 10). The geometric bulking deformation can be estimated by a semi-empirical approach described by Kaiser (2016) using the linear bulking factor (*BF*). The *BF* is defined as the normalized length change in the radial direction to the original length which is used to characterize the bulking-related inelastic deformations within the rock mass (Gao et al. 2019; Kaiser 2020). Accordingly, mining-induced strain around an excavation can be quantified based on a linear *BF* and the average confining pressure as presented in the chart of Fig. 10.

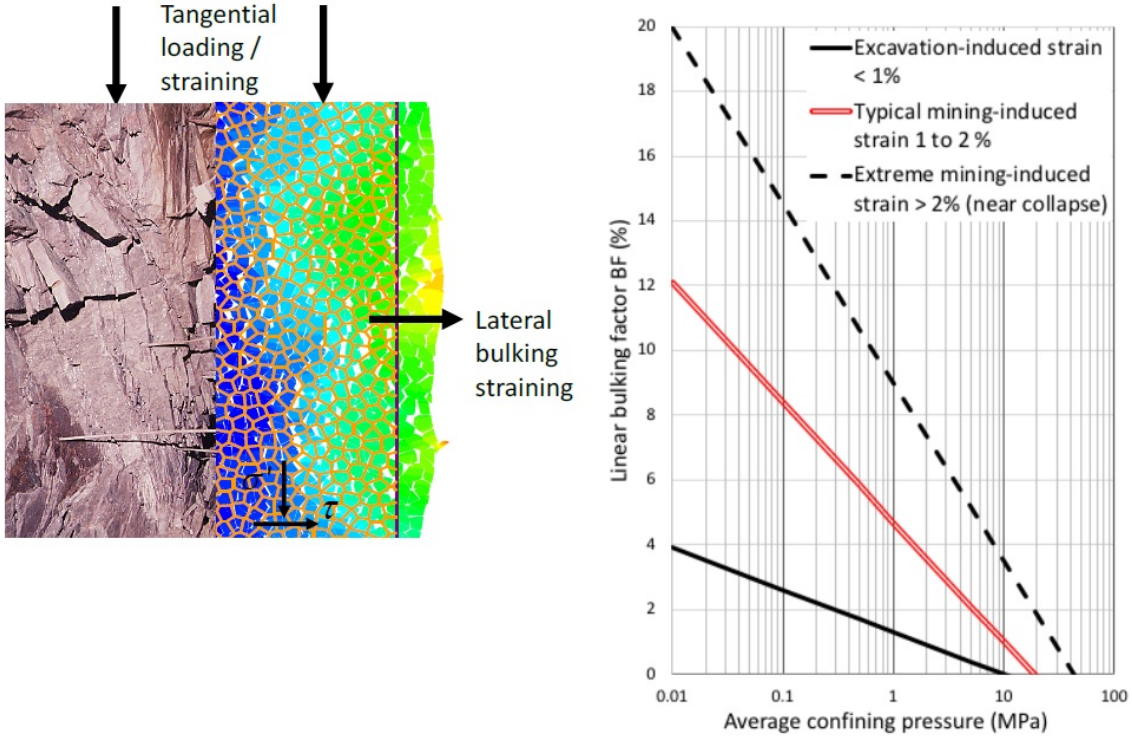

Figure 10- Schematic Illustration of unidirectional rock masses bulking as well as the semi-empirical bulking factor chart (adapted from Kaiser 2020).

3.2.5 Chang's strain-strength criterion

Chang (2006) suggested a strain-strength criterion for rocks formulated as follows (equation 21):

$$\varphi(\varepsilon_{ij}) = k\varepsilon_1 - \varepsilon_v - \varepsilon_c \quad (21)$$

where ε_v is the volumetric strain, ε_1 is the major principal strain, k and ε_c are the parameters controlling the post peak hardening/softening behaviour of rock. Subsequently, Chang (2011) proposed a yielding/damage criterion obtained from the results of laboratory tests which show a linear correlation between the volumetric strain and the major principal strain at yield. The criterion is presented as follows (equation 22) (Hidalgo 2013):

$$\varepsilon_v = k\varepsilon_1 - \varepsilon_c \quad (22)$$

In fact, Chang (2006 and 2011) proposed a method to detect the rock damage by studying the changes of volumetric strains in relation to the major principal strain in the $\varepsilon_v - \varepsilon_1$ space. An engineering tool called strain path analysis (*SPA*) was introduced for this purpose (see Fig. 11). Accordingly, the $\varepsilon_v - \varepsilon_1$ space was categorized into different areas corresponding to different rock loading conditions (Fig. 11). Chang (2011) emphasized the point that ε_v can never be greater than $3\varepsilon_1$ as specified by the area noted by NA in Fig. 11. The starting point of a strain path is typically placed in the elastic domain representing the initial strain state in the rock. The initial strain state, can be subsequently perturbed by rock excavations or mining/tectonic movements. The change in strain path could be characterized by deformation measurements and the strain trace can then be plotted in the $\varepsilon_v - \varepsilon_1$ space (Chang 2011). Accordingly, approaching the strain path to the damage initiation line, indicates the beginning of damage and cracking within the rock. The distance between the actual strain state and the damage initiation line can be used as a measure of the "safety factor". Crossing the strain path over the damage initiation line, indicates that the major principal stress is reaching the peak level and progressive cracking is occurring in the rock mass (Chang 2011). Ultimately, if the strain path follows a very abrupt curve after crossing the damage initiation line, it is very likely that the rock is already experiencing the post-failure stage (Chang 2011).

In terms of applicability, the strain path analysis can be more suitable for direct interpretation of measured deformations during the construction phases of underground excavations. Although, for evaluation of stability state during the design phase, strain paths could be detected by numerical simulations (Chang 2011).

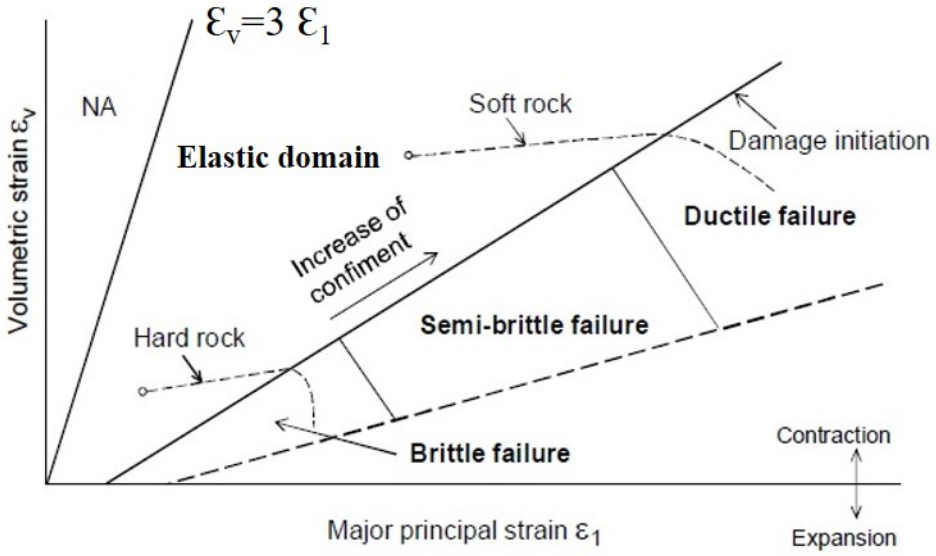

Figure 11- The various defined domains of rock behaviour in ε_v-ε_1 space (adapted from Chang 2011)

3.2.6 Fujii's critical tensile strain criterion

Fujii et al. (1997) proposed the critical tensile strain criterion as presented below (equation 23) to predict the brittle failure of rocks.

$$\varepsilon_3 = \varepsilon_{TC} \qquad (23)$$

where ε_3 is the minimum principal strain (extension), and ε_{TC} is the critical tensile strain. The critical tensile strain is the strain linked to strength at failure (Fig. 12). This criterion was developed based on the results of a series of laboratory tests (e.g. uniaxial compression and Brazilian tests) on cylindrical rock specimens of Kamisunagawa sandstone, Sorachi sandstone, Kimachi sandstone, Kamaishi granodiorite, Shinkomatsu andesite and Inada granite (Fujii et al., 1997). According to this criterion, failure occurs when the minimum principal strain reaches a critical value. The critical values of the lateral and circumferential strains are independent from strain rate (in the range from 0.01 to 4%/min) and from confining pressure (not exceeding 60MPa in the case of Shinkomatsu andesite) (Kwasniewski and Takahashi 2010).

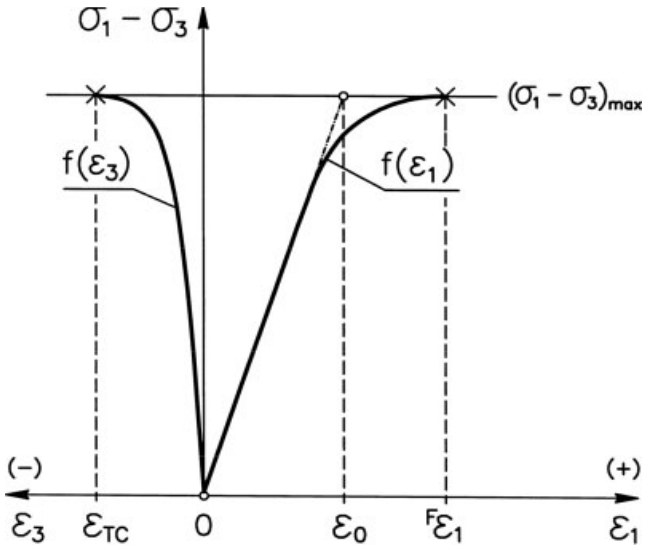

Figure 12- Notion of critical tensile strain (ε_{TC}) (adapted from Kwasniewski and Takahashi 2010).

3.2.7 Mean stress-volumetric strain criterion

Le Roux and Brentley (2018), proposed a stress-strain criterion derived from the linear relationship between the mean stress (σ_m) and volumetric strain (ε_{vol}) around open stopes obtained from plotting the actual data. This criterion was proposed to predict the extent of failure in open stope hanging wall and side walls. Mean stress and volumetric strain can be mathematically expressed as follows (equations 24 and 25):

$$\sigma_m = \frac{\sigma_1 + \sigma_2 + \sigma_3}{3} \qquad (24)$$

$$\varepsilon_{vol} = \varepsilon_1 + \varepsilon_2 + \varepsilon_3 \qquad (25)$$

According to Le Roux and Brentley (2018), the stress-strain criterion (S_{sc}) also referred to as the Dilution Stress Strain Index (DSSI), is formulated as follows (equation 26):

$$S_{sc} = \frac{\sigma_m}{q\varepsilon_{vol}} \qquad (26)$$

where q (GPa), is the slope of the linear trend line between the mean stress and volumetric strain data. By integration of this criterion in numerical analysis the expected failure depth in the hanging wall or sidewalls of excavations can be determined. In fact, if the volumetric strain exceeds the critical value for mean stress, failure will occur (Le Roux and Brentley 2018). As reported by La Roux and Brentley (2018), the predicted failure corresponded very well with the actual observed failure data in twenty-two underground open stope case histories obtained by the CMS (Cavity Monitoring System).

Mean stress-volumetric strain criterion has been used in some recent studies to predict the depth of failure around underground openings under triaxial loading conditions (e.g. Le Roux and Stacey 2017; Le Roux and Brentley 2018; Ahmadinejad et al. 2019).

3.2.8 Plastic damage index (η) criterion

A recently developed strain-based failure criterion by Mohanto and Deb (2019), is the plastic damage index (η), defined as the ratio of the effective plastic strain to the effective total strain. Plastic damage index (η) was introduced along with the strength reduction ratio ($\acute{k}$). The parameter $\acute{k}$ was calculated based on the post-yielding phase of rocks tested under uniaxial compression (Mohanto and Deb 2019). Accordingly, Mohanto and Deb (2019) developed an analytical equation relating the plastic damage index and the strength reduction ratio, obtained by introducing five notional damage classes for the prediction of rib pillar stability (Table 2).

The effective total strain ($\varepsilon^{eff}{}_T$) at stress level (σ^{eff}) in multi-dimensional space are defined as (equations 27 and 28):

$$\varepsilon^{eff}{}_T = \varepsilon^{eff}{}_e + \varepsilon^{eff}{}_p = \frac{\sigma^{eff}}{E} + \varepsilon^{eff}{}_p \qquad (27)$$

$$\sigma^{eff} = \frac{1}{\sqrt{2}}\left\{(\sigma_1-\sigma_2)^2 + (\sigma_2-\sigma_3)^2 + (\sigma_3-\sigma_1)^2\right\}^{1/2} \qquad (28)$$

Where E is the Young's modulus of rock. The effective plastic strain ($\varepsilon^{eff}{}_p$) were also defined as (equation 29):

$$\varepsilon^{eff}{}_p = (\frac{\sqrt{2}}{3})\left\{(\varepsilon^p{}_1-\varepsilon^p{}_2)^2 + (\varepsilon^p{}_2-\varepsilon^p{}_3)^2 + (\varepsilon^p{}_3-\varepsilon^p{}_1)^2\right\}^{1/2} \qquad (29)$$

Equation 29 can be rewritten as the formula below (equation 30) by assuming $\varepsilon^p{}_1 = -\varepsilon^p{}_2/\upsilon$ and $\varepsilon^p{}_1 = -\varepsilon^p{}_3/\upsilon$ as $\varepsilon^p{}_1$ is the plastic strain in axial direction and $\varepsilon^p{}_2$ and $\varepsilon^p{}_3$ are plastic strains in lateral and perpendicular directions of a cylindrical sample respectively.

$$\varepsilon^{eff}{}_p = \varepsilon_p\left[\frac{2}{3}(1+\nu)\right] \qquad (30)$$

where υ is the Poisson's ratio and $\varepsilon^p{}_1$ can be assumed as plastic strain at stress level σ in the post-failure region of UCS test (ε_p). Then, plastic damage index (η) at stress level σ^{eff} could be defined as the ratio of cumulative effective plastic strain ($\varepsilon^{eff}{}_p$) to cumulative effective total strain ($\varepsilon^{eff}{}_T$) as given by equations 31 and 32.

$$\eta = \frac{\varepsilon^{eff}{}_p}{\varepsilon^{eff}{}_T} \qquad (31)$$

$$\eta = \frac{\varepsilon_p\left[\frac{2}{3}(1+\nu)\right]}{\frac{\sigma^{eff}}{E} + \varepsilon_p\left[\frac{2}{3}(1+\nu)\right]} \qquad (32)$$

By considering σ^{eff} equal to σ for the uniaxial compression test since $\sigma_2 = \sigma_3 = 0$, the following formula would be generated (equation 33):

$$\frac{\sigma}{E}\left[a(1-\eta)+\eta\right]=a\varepsilon_T(1-\eta) \qquad (33)$$

Where $a=\frac{2}{3}(1+\nu)$

By dividing both sides of the equation 33 by σ_{ci}, and considering the strength reduction ratio as a ratio of stress level in the plastic region to uniaxial compressive strength (as tested in the laboratory), the following equation would be obtained (equation 34):

$$\kappa=(\frac{E\varepsilon_T}{\sigma_{ci}})(\frac{a}{a(1-\eta)+\eta})(1-\eta) \qquad (34)$$

The relationship between η and ƙ was taken as an indication to classify the damage in rib pillars (under static loading conditions). Table 2 presents the damage classification based on the ranges of plastic damage index, and strength reduction ratio for rocks in the post-yield region. Based on damage severity, five classes were identified as: I, II, III, IV and V from no damage to severe damage. The explanations provided in the Table 2 were obtained based on the expert's opinions as well as the available data on the failure behaviour of rocks under uniaxial and triaxial laboratory tests (Mohanto and Deb 2019).

Table 2- Classification of damage based on plastic damage index and strength reduction ratio (after Mohanto and Deb 2019)

Damage class	Group	Plastic damage index η	Strength reduction ratio ƙ	Explanation
I	No damage	$\eta\leq0.2$	ƙ≥ 0.78	No noticeable damage observed
II	Slight damage	$0.2<\eta\leq0.4$	0.78> ƙ ≥ 0.57	Extension of existing visible cracks or formation of new/fresh visible cracks in roof and / or pillar
III	Moderate damage	$0.4<\eta\leq0.6$	0.57> ƙ ≥ 0.37	Detachment of loosened small rock pieces from the roof and/or pillar
IV	High damage	$0.6<\eta\leq0.8$	0.37> ƙ ≥ 0.19	Fall of rock blocks from the roof and/or pillar
V	Severe damage	$\eta>0.8$	Ƙ < 0.19	Severe damage to the underground openings. May result in the roof fall or collapse of sidewalls

The application of plastic damage index in prediction of rock mass damage / failure has recently been studied by Mohanto and Deb (2019) and Guang et al., (2020).

3.2.9 Displacement / convergence criteria

Displacement measurement is a common approach used in stability assessment of any underground excavation. Displacements occur within the rock mass away from the excavation periphery, while convergence, (i.e., the relative displacement of two points on the boundary of an opening) can be measured on the excavation periphery (Zhang 2006; Brady and Brown 2004; Abdellah 2013). Displacement/convergence indices are used to determine whether the excavation is serviceable or not (Idris et al., 2011). Displacement/convergence indices are generally site specific in terms of their dependence on rock mass stiffness characteristics as well as the intended usage of the underground excavation (Zhang and Mitri, 2008). In some cases, horizontal displacement of excavation walls is measured in terms of wall convergence to provide the relative displacement. The wall convergence ratio (*WCR*) is a non-dimensional index that calculates the percentage of the total excavation wall displacement relative to the span of the excavation (see equation 35):

$$WCR = \frac{W^0 - W^1}{W^0} \times 100\% \qquad (35)$$

where W^0 is the span of excavation; and W^1 is the wall horizontal displacement.

Roof sag (i.e. roof vertical displacement) ratio (*RSR*) as the second criterion can be defined as the ratio of the sagging of roof or back of an excavation (ΔS) to the height of an excavation (W^0) (Zhang and Mitri 2008). Hence (equation 36):

$$RSR = \frac{\Delta S}{W^0} \times 100\% \qquad (36)$$

Floor heave (i.e. floor vertical displacement) ratio (*FHR*) as the third criterion is defined by the ratio of floor heave (Δh) to the height of the excavation (Zhang and Mitri 2008) as (equation 37),

$$FHR = \frac{\Delta h}{W^0} \times 100\% \qquad (37)$$

Floor heave, is an instability condition which occurs where the floor rocks are relatively weak and the material yields under the stresses operating beneath the excavation side walls (Brady and Brown 2004).

Displacement/convergence criteria have been implemented in numerical stability analysis of tunnels (e.g., Panet and Guenot 1982; Vlachopoulos and Diederichs 2009), underground haulage drifts (Zhang and Mitri 2008; Musunuri et al. 2010; Abdellah 2013, Abdellah et al. 2014; Abdellah et al. 2018) and underground open stopes (e.g. Idris et al. 2011; Hidalgo 2013; Badge et al. 2017).

4. DISCUSSION

The main purpose of numerical modeling is to evaluate the state of excavation stability by quantifying the effect of induced stresses and relating different magnitudes of induced stresses to different levels of rock mass damage around an opening void. For underground excavations in deep hard rock mines, the choice of numerical modeling approach includes linear elastic numerical modeling (e.g. Map3D software), and nonlinear elasto-plastic numerical modeling with continuum or discontinuum finite element or finite difference analysis (e.g. software like Abaqus, UDEC, 3DEC, FLAC(3D), Unwedge, RS2/3 and etc.) (Villaescusa 2014).

In linear elastic numerical modeling, a site-specific critical stress level is defined to quantify the damage intensity. The rock mass response below this critical stress level is considered elastic with very little observable damage. However, by increasing the level of overstressing, the damage level increases resulting in development of a potential damage zone around the excavation. Increasing the elastic overstressing beyond the critical level would result in stress-driven failures. The disadvantage of linear elastic modeling is the inability to indicate rock movements, falloffs, or dilution from fault or shear zones (Villaescusa 2014). On the other hand, nonlinear elasto-plastic numerical modeling as a powerful alternative approach, can predict rock mass damage/failure mechanisms for complex mining problems where a potential exists for high levels of deformation and substantial plasticity. In fact, nonlinear numerical analysis is able to compute the displacements, damage and deformations within the rock mass in complex models containing large number of excavations (Bobet 2010; Villaescusa 2014).

Generally, excavation instability in numerical analyses, can be detected by an unacceptable deformation or displacement of the rock mass into the opening void. Displacements and stresses as typical output variables of a numerical simulation, can be compared with pre-defined critical thresholds of various failure criteria (Brady and Brown 2004; Villaescusa 2014). Certain critical thresholds in the forms of displacement (deformation), stress or velocity, or in some cases, a certain volume of rock can be adopted to quantify the intensity of damage or eventual failure (Villaescusa 2014; De Santis 2019). Integration of different failure criteria into the numerical analysis, inevitably includes some limitations and technical considerations which have to be well noted.

First of all, depending on the nature of the problem, the selection of a suitable failure criterion requires that the expected mode of instability be identified based on the rock mass quality and the *in situ* stress state. An appropriate failure criterion among the existing stress-based or strain-based criteria is one that provides a valid explanation of the actual mechanism of instability. To reflect the elastic failure of brittle and hard rock masses (mode M_{11} in Fig. 2), elastic constitutive models should be adopted. Elastic, isotropic models are appropriate for isotropic, homogeneous and continuous rock masses with linear stress-strain behaviour; while the elastic, orthotropic, or transversely isotropic models are suitable to simulate the rock masses that show elastic anisotropy (e.g. laminated rock masses loaded below strength limit). In such cases, the factor of safety can be calculated to reflect the level of instability (Itasca 2014). If a rock mass is subjected to some degree of permanent,

path-dependent deformations (plastic failure), suitable elasto-plastic constitutive models must be selected to determine the extent of yield within the rock mass. For instance, if shear failure is the dominant mode of failure (e.g. M_{33} in Fig. 2), Mohr-Coulomb plasticity model can be used. This constitutive model is suitable to address the yield behaviour of rock materials subjected to shear loading. To characterize the post failure behaviour of rock masses, the strain-hardening/softening models based on variations of the Mohr-Coulomb model properties, or the modified Hoek-Brown model with a stress-dependent plastic flow rule can be used. It should be noted that, even though the Drucker-Prager plasticity model may be useful to model soil behaviour (e.g. soft clays with low friction angles), this model is not recommended for application to rock materials (Itasca 2014).

Aside from the extent of yield or depth of failure criteria, strain-based criteria can also detect the rock mass damage / failure. For instance, the extension strain criterion by Stacey (1981) characterizes the onset of rock fracturing while the criteria by Sakurai (1993) and Chang (2011) are yielding/damage criteria (Hidalgo 2013). However, some questions have been raised regarding the applicability of these conventional strain-based criteria in explaining different failure mechanisms. These arguments are going to be addressed further and should be taken into consideration prior to the selection of such strain-based criteria. In this regard, Stacey made it clear that his extension strain criterion does not have a universal character and it can only address the onset of fracturing in brittle rocks under low confinement (e.g. excavations at shallow depths and/or in the immediate vicinity of underground excavations) (Kwasniewski and Takahashi 2010). Also, the applicability of this criterion in predicting the initiation of failure for all rock types is not yet accepted (Stille et al., 2010). Moreover, Martin (1997) mentioned that it is still not clear what fundamental failure mechanism is explained by this criterion (Ghasemi 2013). In spite of the above-mentioned arguments, some studies support the application of Stacey's criterion, including Martin et al. (1999), Diederichs (2003) and Eberhardt et al. (2004) (as reported by Kwasniewski and Takahashi 2010; Ghasemi 2013; Wesseloo and Stacey 2016). Similar concerns have been raised regarding the applicability of Sakurai's and Chang's methods. In fact, the range of *Rf* suggested by Sakurai (1981) (from 0.05 to 0.8) was reported not to provide a general application since it includes both weak and hard rocks (Hidalgo 2009). Cai (2011) informed that *Rf* could range from 0.1 to 0.3 for hard rock masses and can further increase to 0.4. The Chang's method (2006), also did not clearly indicate how the constants κ and ε_c were determined and under which conditions they apply. Moreover, it was not clear that the plastic deformation determined by Chang's criterion can be interpreted as failure and fallout of rock, or formation of fractures without occurrence of failure (Stille et al., 2010). Also, Fujii's criterion was informed not to be applicable in situations where strain-hardening behaviour is expected (Fujii et al 1997). Another key point is that, these failure criteria are formulated in terms of strain quantities and are all defined according to strength data derived from laboratory tests. For instance, Aydan's criterion is suitable only when the required parameters for numerical analysis are taken from *in situ* tests (Aydan et al., 2012). It can be considered as an advantage of the strain-strength criteria such as Chang's or Sakurai's that the values of volumetric strain, the maximum principal strain and the critical shear strain can be easily determined from laboratory tests. In some cases, the choice of a suitable strain-based failure criterion can be dependent on the field observations. For instance, in some cases, sufficient deformation data might be available by measurement devices (e.g. extensometers), thus making it

possible to set an actual threshold for heave or sagging of a wall. Therefore, using the displacement / convergence indices (e.g. RSR, WCR or FHR), could be considered since they are generally site specific. It is reported that the utilization of displacement / convergence indices to analyze the stability using numerical modeling programs requires prior justifications, as these indices depend on the site-specific rock mass stiffness characteristics, the targeted failure mode of the underground opening, as well as the design and code requirement (Zhang and Mitri, 2008).

If the brittle failure of the rock mass is required to be evaluated, the choice of stress-based brittle failure criteria (such as BSR) are highly recommended. In numerical analysis programs such as FLAC, an embedded programming language code (e.g. FISH code for FLAC software) is designed to facilitate the integration of new variables and functions. As an example, BSR function can be coded within the FISH language using the maximum shear stress (one of the outputs in FLAC) in the model (Shnorhokian et al., 2015; Heidarzadeh et al., 2018a). About using the BSR criterion, it should be taken into consideration that it provides more definite results in a heterogeneous rather than homogeneous rock masses. This is because the effect of a differential stress value on BSR could change from one formation to the other having different strength properties (Shnorhokian 2018). If numerical modeling programs are incapable of directly defining the *s*-shaped or tri-linear failure envelopes required for rock brittle failure, the *s*-shaped peak strength envelope could be approximated by adopting appropriate Hoek–Brown (or Mohr–Coulomb) parameters (Kaiser 2020). As mentioned by Kaiser (2020) best practice in such cases could be to ignore the common Hoek–Brown parameter tables (Hoek et al. 1995) and to adopt a representative mean UCS value and a high, best fit m_i value (Kaiser 2020). In addition to shear-related instabilities, the possibility of low confinement compressive or tensile failure can be detected by the stress concentration ratio and tensile strength-to-stress ratio respectively. In a stress concentration criterion, the comparison of the major principal induced stress with the UCS of intact rock could only be valid in immediate vicinity of an opening face, since the confinement (or minor principal stress) is zero (Shnorhokian et al., 2015; Heidarzadeh et al. 2018b). As a diagnosis indication in numerical modeling, if the *SCF* is more or less uniform around the excavations periphery, such excavation is considered more stable (Shnorhokian et al., 2015). This criterion can also be used in linear elastic numerical modeling as an indicator of potential failure (Zhang and Mitri 2008).

To avoid misinterpretation of numerical modeling results, the difference between yielded and failed rock masses should be clearly stated. As noted before, rock mass around an excavation void could actually be yielded under the loading conditions but yet unremoved, due to e.g. the local arched shape of the span holding up the yielded rock (Villaescusa 2014). In continuum numerical modeling programs such as FLAC3D, plastic indicators (e.g. plastic strain) display the zones in which the stresses satisfy the yield criterion. This indication normally signifies the occurrence of plastic flow; however, it is possible for an element to remain on the yielded area without any major flow taking place. Also, the plastic indicators are capable of identifying the current yielded zones as well as the zones that have failed earlier in the model run, but the stresses are currently below the yield surface. In fact, at the beginning of a simulation, some zones can be subjected to initial plastic flow but subsequent stress redistribution can unload the yielding zones so that their stresses no longer exceed the yield surface. In this regard, evolution of the stress state in the model over the duration of a simulated mining activity should be considered

accurately, as changes in the stress level may lead to changes in failure modes (Kaiser 2020). For instance, relaxation of an excavation wall could alter the failure mode from M_{22} or $_{23}$ to M_{21} or $_{31}$; while an increase in extraction ratio could result in changing from M_{22} or $_{32}$ to M_{23} or $_{33}$ (See Fig. 2) (Kaiser 2020). Therefore, it is important to consider the entire pattern of plasticity indicators to see whether a failure mechanism has developed. Development of a failure mechanism is concluded if there is a connecting line of active plastic zones that join two separate surfaces and if the velocity plot also shows motion corresponding to the same mechanism (Itasca 2014; Villaescusa 2014). Actually, velocity (i.e. displacement per mining step) can be taken as an upper-bound indicator for instability, as all grid points having high velocity should supposedly be assumed unstable even if the rock is undamaged (e.g., a moving rock mass bounded by structure). While, plastic strain (i.e. rock damage) can be considered as a lower-bound indicator of instability, as rock mass can be damaged, but may still be stable if the velocity is low (Cepuritis et al., 2010; Villaescusa 2014). As a rule of thumb, points in the numerical model that show large velocities could be expected to have a very high likelihood of instability. While, the points that are located at the excavations surface displaying high levels of plastic strain and low levels of confinement, are expected to fail in the form of falloffs (Villaescusa 2014).

As a final remark, the reliability of a failure criterion can be accurately assessed by using the criterion to simulate an observed failure. In fact, confirmation of underground design reliability can be obtained through back analyzing quantitative damage / failure criteria, such as depth of failure (Ghasemi 2013; Villaescusa 2014). Back-analysis can also be used to calibrate any given failure criteria. Moreover, back analyzing of an observed case of failure, helps in generating new empirical relationships between the key parameters defining the state of stability. In this regard, Cepuritis et al. (2010) reported a relationship between maximum velocity during stope extraction (regardless of plastic strain) and the percentage of “unstable” points around a stope. Furthermore, a relationship between plastic strain during stope extraction (regardless of velocity) and the percentage of “unstable” points was also obtained. Villaescusa (2014) suggested this criterion as a reasonable predictor of falloff occurrence, as the rock masses with this corresponding level of plastic strain and velocity, would almost certainly unravel if unconfined and exposed.

5. CONCLUSION

In this paper, an in-depth review is presented on the theoretical fundaments and applicability of the most common failure criteria used in numerical stability analysis of underground excavations. Several stress-based and strain-based failure criteria were studied both in terms of theory and practice. The focus of this study was on the criteria used in continuum numerical analysis. An effort was made to suggest more suitable and efficient criteria regarding different failure mechanisms.

As concluding remarks, it was emphasized that the choice of failure criteria should be dependent on the anticipated mode of failure. In addition, the field conditions of the problem should be considered as a leading factor. Even though employment of stress-based

failure criteria is more common in numerical analysis, their usage is not always reasonable and / or justified. Strain-based failure criteria can be employed in cases where the selection of appropriate constitutive models for rock is not convenient maybe due to the lack of enough reliable data, and/or in the cases where, the evaluation of rock deformations is more convenient using appropriate measurement devices.

The quantification of the state of underground instability can be successfully achieved by implementing suitable failure criteria in numerical analysis tools. For underground excavations in deep hard rock mines, nonlinear elasto-plastic numerical modeling with continuum or discontinuum finite element or finite difference analysis could be the best choice. In this paper, some useful tips and remarks were also provided regarding the numerical implementation of different failure criteria. In this regard, it was noted that using the embedded programming language codes in numerical programs (e.g. FISH code for FLAC software), could be helpful for integrating failure criteria. Finally, it was recommended in this paper, to assess the reliability of the failure criteria by using them to simulate an observed case of failure. Back-analysis can also be useful in the calibration of any given failure criteria. It is worth to point out that considering the theoretical and practical issues addressed in this paper, would make the numerical stability analysis of underground excavation, a more convenient task for the underground rock engineers.

ACKNOWLEDGEMENT

This study was funded by a Grant from Natural Sciences and Engineering Research Council of Canada (NSERC) (RDCPJ520428-17).

REFERENCES

Abdellah W. (2013). Geotechnical risk assessment of mine haulage drifts during the life of a mine plan. PhD thesis, McGill University, Montreal, Canada.

Abdellah W, Raju GD, Mitri HS, Thibodeau D. (2014). Stability of underground mine development intersections during the life of a mine plan. International Journal of Rock Mechanics and Mining Sciences; 72:173–181.

Abdellah, W. (2015). Numerical modelling stability analyses of haulage drift in deep underground mines. Journal of Engineering Science, 43 (1), pp. 71-81

Abdellah, W. R., Ali, M. A., & Yang, H. S. (2018). Studying the effect of some parameters on the stability of shallow tunnels. Journal of Sustainable Mining, 17(1), 20-33.

Aglawe, JP. (1999). Unstable, violent failure around underground openings in highly stressed ground. PhD thesis, Queen's University at Kingston.

Ahmadinejad, A. Rahimzadeh Kivi, I. Ameri, M.J. (2019). Experimental Study of the Hydro-Mechanical Response of Tight Sarvak Carbonates to Hydrostatic and Deviatoric Stress Changes. American Rock Mechanics Association. 53rd U.S. Rock Mechanics/Geomechanics Symposium, 23-26 June, New York City, New York, US.

Ajalloeian, R., Moghaddam, B. & Azimian, A. (2017). Prediction of Rock Mass Squeezing of T4 Tunnel in Iran. *Geotech Geol Eng* **35,** 747–763 doi:10.1007/s10706-016-0139-y.

Aydan, Ö., Akagi, T. and Kawamoto, T. (1993). The Squeezing potential of rocks around tunnels – theory and prediction. Rock Mechanics and Rock Engineering, 26(2): 137- 163.

Aydan, Ö., Tokashiki, N., & Geniş, M. (2012). Some Considerations on Yield (Failure) Criteria In Rock Mechanics. The 46th US Rock Mechanics / Geomechanics Symposium held in Chicago, IL, USA, 24-27 June 2012.

Bagde, M.N. Sangode, A.G. Jhanwar, J.C. (2017). Evaluation of Stoping Parameters through Instrumentation and Numerical Modelling in Manganese Mine in India: A Case Study, Procedia Engineering, Volume 191, Pages 10-19, ISSN 1877-7058.

Barla, G. (1995). Squeezing rocks in tunnels. ISRM News Journal, 2(3), pp.44-49.

Beck, D. A. and Duplancic, P. (2005). Forecasting performance and achieving performance indicators in high stress and seismically active mining environments. In Y. Potvin and M. Hudyma (eds.), Controlling Seismic Risk, Proceedings of the Sixth International Symposium on Rockburst and Seismicity in Mines, Perth, Western Australia, Australia, 9–11 March, pp. 409–417.

Bewick, R.P. (2008). Effects of anisotropic rock mass characteristics on excavation stability. Master's thesis. Laurentian University. School of Graduate Studies. Ontario, Canada.

Bewick, R.P., Kaiser, P.K. & Amann, F. (2019). Strength of massive to moderately jointed hard rock masses. Rock Mechanics and Geotechnical Engineering, 11(3): 562-575 https://doi.org/10.1016/j.jrmge.2018.10.003

Bieniawski, Z.T. (1967). Mechanism of brittle rock fracture. Part I. Theory of the fracture process. International Journal of Rock Mechanics and Mining Sciences and Geomechanical Abstracts, 4(4): 395-406.

Bobet, A. (2010). Numerical methods in geomechanics. The Arabian Journal for Science and Engineering, 35(1B), pp.27–48.

Brady, B.H.G. and Brown, E.T. (2004). Rock mechanics for underground mining. Springer, 3rd edition, The Netherlands, 628 p.

Brady, B.H.G. and Lorig, L. (1988) 'Analysis of rock reinforcement using finite difference methods', Comp. Geotech., Vol. 5, No. 2, pp.123–149.

Cai, M., Kaiser, P.K., Tasaka, Y., Maejima, T., Morioka, H., Minami, M., (2004). Generalized crack initiation and crack damage stress thresholds of brittle rock masses near underground excavations. Int. J. Rock Mech. Min. Sci. 41,833–847.

Cai, M. (2011). Rock mass characterization and rock property variability considerations for tunnel and cavern design. Rock Mechanics and Rock Engineering; 44(4), 379-399.

Cai, M. Kaiser, P.K. (2018). Rockburst support reference book, Rockburst phenomenon and support characteristics. MIRARCO—mining innovation. 1 Laurentian University, Sudbury

Castro LAM, Bewick RP, Carter TG. (2012). An overview of numerical modelling applied to deep mining. In: Azevedo R, editor. Innovative numerical modelling in geomechanics. London: CRC Press — Taylor & Francis Group; p. 393–414.

Cepuritis, P. M., Villaescusa, E., and Lachenicht, R. (2007). Back analysis and performance of Block A long hole open stopes—Kanowna Belle Gold Mine. In E. Eberhardt, D. Stead, and T. Morrison (eds.), Rock Mechanics: Meeting Society's Challenges and Demands, Proceedings of the First Canada—US Rock Mechanics Symposium, Vancouver, Canada, 27–31 May, pp. 1431–1439.

Cepuritis, P. M., Villaescusa, E., Beck, D. A., and Varden, R. 2010. Back analysis of over-break in a longhole open stope operation using non-linear elasto-plastic numerical modelling. In Proceedings of the 44th US Symposium of Rock Mechanics and Fifth Canada—US Rock Mechanics Symposium, Salt Lake City, UT, 27–30 June, Paper ARMA 10–124, 11pp.

Chang, Y. (2006). Rock strain-strength criterion and its application. In: Leung, C.F. and Zhou, Y.X. (Eds.): 4th Asian Rock Mechanics Symposium, ISRM International Symposium on Rock Mechanics in Underground Constructions, World Scientific Publishing Co. Pte. Ltd., Singapore, November 8-11 2006, ISBN 981-270-437-X.

Chang, Y. (2011). Applications of strain based damage criterion in geotechnical engineering. In: Qian, Q. and Zhou, Y. (Eds.): 12th ISRM International Congress on Rock Mechanics. Harmonising Rock Engineering and the Environment, Taylor & Francis Group, Beijing, China, October 16-21 2012, ISBN 978-0-415-80444-8.

Chen, D. Chen, J. Zavodni, ZM. (1983). Stability analysis of sublevel open stopes at great depth. In: Proceedings of the 24th U.S. Symposium on Rock Mechanics (USRMS).

Cundall, P. Carranza-Torres, C. Hart, R. A new constitutive model based on the Hoek-Brown criterion. In: Brummer et al. (Eds.), FLAC and Numerical Modeling in Geomech. ISBN 90 5809 581 9.

De Santis, F. 2019. Rock mass mechanical behaviour in deep mines: in situ monitoring and numerical modelling for improving seismic hazard assessment. PhD thesis, University of Lorraine.

Diederichs MS. (1999). Instability of hard rock masses: the role of tensile damage and relaxation. PhD Thesis. Waterloo, Ontario: University of Waterloo.

Diederichs, M. S., (2003), Rock fracture and collapse under low confinement conditions. Rock Mech. Rock Engng, Vol. 35 (5), pp 339 – 381.

Diederichs, M.S. (2007). Mechanistic interpretation and practical application of damage and spalling prediction criteria for deep tunnelling. Canadian Geotechnical Journal, 44(9), pp.1082-116.

Drucker, D. C. Prager, W. (1952). Soi! Mechanics and Plastic Analysis or Limit Design. Quarterly of Applied Methematics, 10, pp 157-165.

Eberhardt, E., Stead, D., Stimpson, B. and Read, R.S. (1998). Identifying crack initiation and propagation thresholds in brittle rock. Canadian Geotechnical Journal, 35(2): 222-233.

Eberhardt, E., Spillmann, T., Maurer, H., Willenberg, H., Loew, S., Stead, D., (2004). The Randa Rockslide Laboratory: Establishing brittle and ductile instability mechanisms using numerical modelling and microseismicity. 9th International Symposium of Landslides, Rio de Janerio, June 28 – July 2, A. A Balkema, Leiden, pp. 481 – 487.

Edelbro, C. (2003) Rock mass strength - A review. Technical report 2003:16, Luleå University of Technology, Division of rock mechanics.

Edelbro, C. (2008). Strength, fallouts and numerical modelling of hard rock masses. PhD thesis. Luleå University of Technology, Department of Civil, Mining and Environmental Engineering Division of Mining and Geotechnical Engineering. Sweden.

Edelbro, C., Sandström, D. (2009). Interpretation of failure and fallouts based on numerical modelling of an underground mine stope. Paper presented at the International Symposium on rock mechanics- Sinorock 2009.

Fujii Y, Kiyama T, Ishijima Y (1997) Condition insensitive damage indicator for brittle rock. Int J Rock Mech Min Sci 34(3–4):086

Gao, F., Kaiser, P.K., Stead, D., Eberhardt, E. & Elmo, D. 2019. Strainburst phenomena and numerical simulation of self-initiated brittle rock failure. International Journal of Rock Mechanics and Mining Sciences, 116: 52-63.

Ghasemi, Y. (2012). Numerical studies of mining geometry and extraction sequencing in Lappberget, Garpenberg. Master's thesis. Lulea University of Technology. Sweden.

Golchinfar, N. (2013). Numerical modeling of brittle rock failure around underground openings under static and dynamic stress loadings. PhD thesis. Laurentian University. School of Graduate Studies. Ontario, Canada.

Gomez-Hernandez, J. Kaiser, P. K. (2003). Modeling Rock Mass Bulking around Underground Excavations. Paper presented at the *ISRM 2003-Technology Roadmap for Rock Mechanics*, South African Institute of Mining and Metallurgy, Vol.1, pp.389-395.

Guang, H. Lun, G. Xuefei, S. Zhenning, L. Xi-Yuan, W. (2020). Numerical investigation on flexural performance of retrofitted tunnel lining with short bolts and steel-plate, Tunnelling and Underground Space Technology, Volume 95, 103152, ISSN 0886-7798, https://doi.org/10.1016/j.tust.2019.103152.

Hadjiabdolmajid V, Kaiser PK, Martin CD (2002) Modelling brittle failure of rock. Int J Rock Mech Min Sci 39:731–741.

Heidarzadeh, S. (2018). Probabilistic stability analysis of open stopes in sublevel stoping method by numerical modeling. PhD thesis. Université du Québec à Chicoutimi, Quebec, Canada.

Heidarzadeh S, Saeidi A, Rouleau A. (2018a). Assessing the effect of open stope geometry on rock mass brittle damage using a response surface methodology. International Journal of Rock Mechanics and Mining Sciences; 106:60–73.

Heidarzadeh S, Saeidi A, Rouleau A. (2018b). Evaluation of the effect of geometrical parameters on stope probability of failure in the open stoping method using numerical modeling. International Journal of Mining Science and Technology.

Heidarzadeh, S., Saeidi, A. & Rouleau, A. (2019). Use of Probabilistic Numerical Modeling to Evaluate the Effect of Geomechanical Parameter Variability on the Probability of Open-Stope Failure: A Case Study of the Niobec Mine, Quebec (Canada). Rock Mech Rock Eng doi:10.1007/s00603-019-01985-4.

Hidalgo, P. (2009). Deformation and failure of hard rock under laboratory and field conditions. PhD thesis. Lulea university of technology, Sweden.

Hidalgo, P. (2013). Deformation and failure of rock. Befo report 13. Lulea university of technology. ISSN 1104 – 1773. Stockholm, Sweden.

Hoek, E. Brown, E. T. (1980). Empirical Strength Criterion for Rock Masses. J Geotech. Engng Div., ASCE, Vol. 106 ((GT9)), pp. 1013-1035.

Hoek E., Kaiser, P.K. & Bawden, W.F. (1995). Rock Support for Underground Excavations in Hard Rock. A.A. Balkema, Rotterdam, 215 p.

Hoek, E. and Marinos, P. (2000). Predicting tunnel squeezing problems in weak heterogeneous rock masses. Tunnels and tunneling international, 32(11), pp.45-51.

Hoek, E. Martin, C.D. (2014). Fracture initiation and propagation in intact rock — a review. J. Rock Mech. Geotech. Eng., 6 (4), pp. 287-300

Hutchinson, D.J. Diederichs, M.S. (1996) Cable bolting in Underground Mines. BiTech Publishers Ltd. ISBN 0-921095-37-6. Vancouver, Canada.

Idris MA, Saiang D, Nordlund E. (2011). Probabilistic analysis of open stope stability using numerical modelling. International Journal of Mining and Mineral Engineering; 3(3):194–219.

Idris MA. (2014). Probabilistic stability analysis of underground mine excavations. PhD thesis, Lulea University of Technology, Lulea, Sweden.

Idris, MA, Saiang, D, Nordlund, E. (2015). Stochastic assessment of pillar stability at Laisvall mine using Artificial Neural Network. Tunn Undergr Sp Technol. 49:307–319.

Itasca Consulting Group, Inc. (2014). Manual of FLAC3D — Fast Lagrangian Analysis of Continua in Three Dimensions, Ver. 5.0. Minneapolis: Itasca.

Jethwa, J.L., Singh, B. and Singh, B., (1984). Estimation of ultimate rock pressure for tunnel linings under squeezing rock conditions—a new approach. In Design and Performance of Underground Excavations: ISRM Symposium—Cambridge, UK, 3–6 September 1984 (pp. 231-238). Thomas Telford Publishing.

Kaiser PK, Diederichs MS, Martin CD, Sharp J, Steiner W. (2000). Underground works in hard rock tunneling and mining. Keynote lecture at GeoEng2000, Melbourne, Australia, Technomic Publishing Co. vol. 1. p. 841–926.

Kaiser, P.K. (2016). Ground Support for Constructability of Deep Underground Excavations - Challenge of managing highly stressed brittle rock in civil and mining projects. ITA Sir Muir Wood lecture of Intern. Tunneling Association at World Tunneling Congress, San Francisco, 33 p. www.ita-aites.org or http://www.mirarco.org/grc/#ert_pane1-4.

Kaiser, P.K. (2020). From common to best practices in underground rock engineering. Rock mechanics for natural resources and infrastructure development-Fontoura, Rocca & Pavon Mendoza (Eds). Taylor & Francis Group, London, ISBN 978-0-367-42284-4.

Kumar, P. (2003). Development of Empirical and Numerical Design Techniques in Burst Prone Ground at the Red Lake Mine. Master's Thesis, University of British Columbia, Vancouver, BC, Canada.

Kwasniewski M, Takahashi M (2010) Strain-based failure criteria for rocks: state of the art and recent advances. In: Zhao J, Labiouse V, Dudt JP, Mathier JF (eds) Rock mechanics in civil and environ- mental engineering. Taylor & Francis Group, London, pp 45–56.

Ladanyi, B. (1974) Use of the long-term strength concept in the determination of ground pressure on tunnel linings. Advances in rock mechanics. Proceedings of the third Congress, International Society of Rock Mechanics, 1974. Denver: National Academy of Sciences, 1150–6

Lade, P. V., & Jackobsen, K P. (2002). Incrementalization of a Single Hardening Constitutive Model for Frictional Materials. Int. J. Numer. Anual. Meth. Geomech, Vol. 26, pp. 647-659.

Le Roux, PJ, and TR Stacey. (2017). Value Creation in a Mine Operating with Open Stoping Mining Methods. Journal of the Southern African Institute of Mining and Metallurgy, 117(2), 133-142

Le Roux, PJ, and Brentley, KR. (2018). Simulation of fracture propagation depth and failure in long hole open stoping. Geomechanics and Geodynamics of Rock Masses – Litvinenko (Ed.) 2018 Taylor & Francis Group, London, ISBN 978-1-138-61645-5.

Liang, Z.Z.; Gong, B.; Li, W.R. (2019). Instability analysis of a deep tunnel under triaxial loads using a three-dimensional numerical method with strength reduction method. Tunn. Undergr. Space Technol. 86, 51–62.

Louchnikov, V. (2011). Simple calibration of the extension strain criterion for its use in numerical modelling. In: Potvin Y (ed) Strategic vs tactical approaches in mining. Australian Centre for Geomechanics, Perth, pp 85–96

Mah, S.G.L. (1997). Quantification and prediction of wall slough in open stope mining methods. Master's thesis. University of British Columbia, Department of mining and mineral process engineering. Vancouver, Canada.

Martin, C.D. (1997). Seventeenth Canadian geotechnical colloquium: the effect of cohesion loss and stress path on brittle rock strength. *Canadian Geotechnical Journal*, ***34***(5), pp. 698-725.

Martin CD, Kaiser PK, McCreath DR. (1999). Hoek-Brown parameters for predicting the depth of brittle failure around tunnels. Can Geotech J 36(1):136–51.

Martin, C.D. (2019). Stress-induced fracturing (Spalling) around underground excavations: Laboratory and in-situ observations. ISRM on-line lecture, https://www.isrm.net/gca/?id=1359.

Mathews, K.E., Hoek, E., Wyllie, D.C. and Stewart, S.B.V. (1981) Prediction of Stable Excavations for Mining At Depth Below 100 Meters in Hard Rock, Report No. DSS Serial N. OSQ80-00081, DSS File No. 17SQ.23440-0-9020, Department Energy, Mines and Resources, Ottawa.

Mitri, H. S. (2007). Assessment of horizontal pillar burst in deep hard rock mines. International Journal of Risk Assessment and Management 7 (No. 5): 695-707.

Mohanto, S., Deb, D. (2019). Prediction of Plastic Damage Index for Assessing Rib Pillar Stability in Underground Metal Mine Using Multi-Variate Regression and Artificial Neural Network Techniques. *Geotech Geol Eng* doi:10.1007/s10706-019-01065-y

Musunuri, A., H. S. Mitri, et al. (2010). Stochastic analysis of haulage drift stability using numerical modelling In Proc ISRM International Symposium 2010 and 6th Asian Rock Mechanics Symposium-Advances in Rock Engineering 23-27 October, New Delhi, India.

Naung, N., Sasaoka, T., Shimada, H., Hamanaka, A., Wahyudi, S. and Pisith, M. (2018) Stability Assessment of Open Stope under Overlaying Mined-Out Regions at Modi Taung Gold Mine, Myanmar. International Journal of Geosciences, 9, 547-571. https://doi.org/10.4236/ijg.2018.99032

Obert, L., Duvall, W. 1., & Merril, R. H. (1960). Design of Underground Openings in Competent Rock. *Bulletin: US Bureau of Mines*, 587, pp. 9.

Oniyide, G.O. Idris, M.A. (2019). Numerical modelling of the effect of temperature variation on stope stability in Bushveld Igneous Complex. Mining and Mineral Deposits; Volume 13 (2019), Issue 2, pp. 121-131.

Pan, XD. Hudson, JA. (1988). A simplified three-dimensional Hoek- Brown yield criterion. In: Romana M (ed) Rock mechanics and power plants. Balkema, Rotterdam, pp 95–103

Panet M, Guenot A (1982) Analysis of Convergence behind the face of a tunnel. International Symposium "Tunneling 82". Brighton, pp 197–204.

Perras, M.A., and Diederichs, M.S. (2016). Predicting excavation damage zone depths in brittle rocks. Journal of Rock Mechanics and Geotechnical Engineering, 8(1): 60-74.

Potvin, Y. (1988) Empirical Open Stope Design in Canada. PhD thesis, University of British Columbia, Vancouver, Canada.

Priest, SD. (2005). Determination of shear strength and three-dimensional yield strength for the Hoek-Brown criterion. Rock Mech Rock Eng 38(4):299–327

Purwanto, A. Shimada, H. Sasaoka, T. Wattimena, R. K., & Matsui, K. (2013). Influence of Stope Design on Stability of Hanging Wall Decline in Cibaliung Underground Gold Mine. International Journal of Geosciences, 4, 1-8. DOI: http://dx.doi.org/10.4236/ijg.2013.410A001

Roache, B. (2016). Mining in extreme squeezing conditions at the Henty mine. In Proceedings of Eighth International Symposium on Ground Control in Mining and Underground Construction. Lulea University, Sweden.

Sahebi, A. Hossein, J. Ebrahimi, M. (2010). Stability analysis and optimum support design of a roadway in a faulted zone during longwall face retreat - case study: Tabas Coal Mine, in Aziz, N (ed), 10th Underground Coal Operators' Conference, University of Wollongong & the Australasian Institute of Mining and Metallurgy, 88-96.

Sakurai S. (1981). Direct strain evaluation technique in construction of underground opening. In: The 22nd U.S. Symposium on Rock Mechanics, USRMS, Cambridge, MA, June 29- July 2 1981, Paper 81-0278.

Sakurai, S., Kawashima, I. and Otani, T. (1993). A criterion for assessing the stability of tunnels. In: Ribeiro, L., Sousa, E. and Grossmann, N.F. (Eds.): ISRM International Symposium, EUROCK 1993, Balkema, Rotterdam, June 21-24 1993, Lisboa, Portugal, pp. 969-973.

Sakurai, S., Kawashima, I. & Otani, T. (1995). A criterion for assessing the stability of tunnels. In L. Ribeiro e Sousa & N.F. Grossmann (eds), Safety and Environmental Issues in RockEngineering; Proc. ISRMIntern. Symp. EUROCK ’93, Lisbon, 21–24June 1993, Vol. 2, 969-973. Rotterdam: Balkema.

Sepehri, M. (2016). Finite Element Analysis Model for Determination of In-situ and Mining Induced Stresses as a Function of Two Different Mining Methods Used at Diavik Diamond Mine. PhD thesis. University of Alberta, Alberta, Canada.

Shnorhokian S, Mitri HS, Moreau-verlaan L. (2015). Stability assessment of stope sequence scenarios in a diminishing ore pillar. International Journal of Rock Mechanics and Mining Sciences; 74:103–118.

Shnorhokian S, MacNeil B, Mitri H. (2018). Volumetric analysis of rock mass instability around haulage drifts in underground mines. Journal of Rock Mechanics and Geotechnical Engineering; Volume 10, Issue 1, Pages 60-71.

Singh, B. Goel, R.K. Jethwa, J.L. Dube, A.K. (1997). Support pressure assessment in arched underground openings through poor rock masses, Engineering Geology, Volume 48, Issues 1–2, Pages 59-81, ISSN 0013-7952, https://doi.org/10.1016/S0013-7952(97)81914-X.

Singh, M., Singh, B. and Choudhari, J. (2007). Critical strain and squeezing of rock mass in tunnels. Tunnelling and underground space technology, 22(3), pp.343-350.

Souley, M., Su, K., Ghoreychi, M., Armand, G., (2003). Constitutive models for rock mass: numerical implementation, verification and validation. In: Brummer et al. (Eds.), FLAC and Numerical Modeling in Geomech. ISBN 90 5809 581 9.

Stacey, T.R. (1981). A simple extension strain criterion for fracture of brittle rock. International Journal of Rock Mechanics and Mining Sciences and Geomechanics Abstracts, 18(6): 469-474.

Steffanizzi, S. Barla, G. Kaiser, P.K. (2007). Numerical modelling of strain driven fractures around tunnels in layered rock masses. In: Ribeiro, Olalla and Grossmann (eds) Proc. 11th Int. Cong. Int. Soc. Rock Mech. Taylor and Francis Group, London, pp 971–974

Stille, H., Zetterlund, M., Perez, K., Bagheri, M. (2010). The observational method. Rock engineering research foundation. Befo report 95. ISSN 1104-1773. Stockholm, Sweden.

Suorineni, F. T. (2010). The stability graph after three decades in use: Experiences and the way forward. International Journal of Mining, Reclamation and Environment, 24(4), 307-339.

Ulusay, R. Hudson, JA. (2007). The Complete ISRM Suggested Methods for Rock Characterization, Testing and Monitoring: 1974 - 2006, International Society for Rock Mechanics, Lisbon.

Valley, B. Kaiser, P.K. Duff, D. (2010). Consideration of uncertainty in modelling the behaviour of underground excavations. Deep Mining: 5th International Seminar on deep and high stress mining. Santiago, Chile. Australian Centre for Geomechanics, In: Van Sint Jan, M., Potvin, Y. (Eds.): 423-436.

Villaescusa E. (2014). Geotechnical design for sublevel open stoping. CRC Press.

Vlachopoulos, N. and Diederichs, M.S. (2009). Improved longitudinal displacement profiles for convergence confinement analysis of deep tunnels. Rock Mechanics and Rock Engineering, 42(2): 131-146.

Wei, W. (2010). Numerical modelling study of rock support system for deep mine haulage drift. Master's thesis. McGill University, department of mining and materials engineering. Montreal, Canada.

Wengang, Z. (2013). Probabilistic risk assessment of underground rock caverns. PhD thesis. Nanyang technological university. School of civil and environmental engineering. Singapore.

Wesseloo, J., Stacey, T.R. (2016). A Reconsideration of the Extension Strain Criterion for Fracture and Failure of Rock. *Rock Mech Rock Eng* **49,** 4667–4679 doi:10.1007/s00603-016-1059-0.

Zhang, Y. (2006). Nonlinear Rock Mass Behaviour and Application to Stability of Underground Haulage Drift. Master's thesis. McGill University, Department of Mining, Metals and Materials Engineering. Canada.

Zhang, W.G. and Goh, A.T.C. (2012). Reliability assessment on ultimate and serviceability limit states and determination of critical factor of safety for underground rock caverns. Tunn. Undergr. Sp. Tech., 32, 221-230.

Zhang, L. Zhu, H. (2007). Three-dimensional Hoek-Brown strength criterion for rocks. J Geotech Geoenvir Eng ASCE 133(9):1128– 1135.

Zhang Y, Mitri HS. (2008). Elastoplastic stability analysis of mine haulage drift in the vicinity of mined stopes. International Journal of Rock Mechanics and Mining Sciences; 45(4):574–593.